Impact of Airborne Radio Occultation Observations on Atmospheric River Precipitation Forecasts on the US West Coast

Jennifer S. Haase, Michael J. Murphy Jr., Bing Cao, Shu-Hua Chen*, Minghua Zheng, F. Martin Ralph

*UC Davis

SCRIPPS INSTITUTION OF OCEANOGRAPHY
UC San Diego

Overview

- Motivation: Example from Oroville Dam in California
- GPS and Galileo data from atmospheric river flights in 2018
- Use of ARO for WRF - GSI assimilation experiment validation*
- Comparison of GPS & Galileo increment from a WRF 3Dvar data assimilation experiment
- Spire RO data for an atmospheric river event*
- Future perspectives – polarimetric*, Strateole-2*
- Open postdoc position at beautiful Scripps by the beach

High stakes forecasting challenges in AR events

- Reservoir managers benefit from improved forecasting in order to keep more water in reservoirs for warm-season demand without endangering downstream populations during cool-season rainfall.
- 180,000 residents were evacuated in the Oroville Dam crisis, caused by the unusually high number of storms (49) and cumulative precipitation (2.5 times prevous record high)
- Extreme precipitation occurred 12 February 2017 (AR 5 on the AR scale; Ralph et al., 2019, BAMS).
- This motivates the effort for targeted observations

to improve quantitative precipitation forecast accuracy

http://www.water.ca.gov/spotlight_archive/

See Corringham et al. 2019 Sci. Advances for a review of damages caused by AR storms.

Atmospheric river event 27-29 January 2018

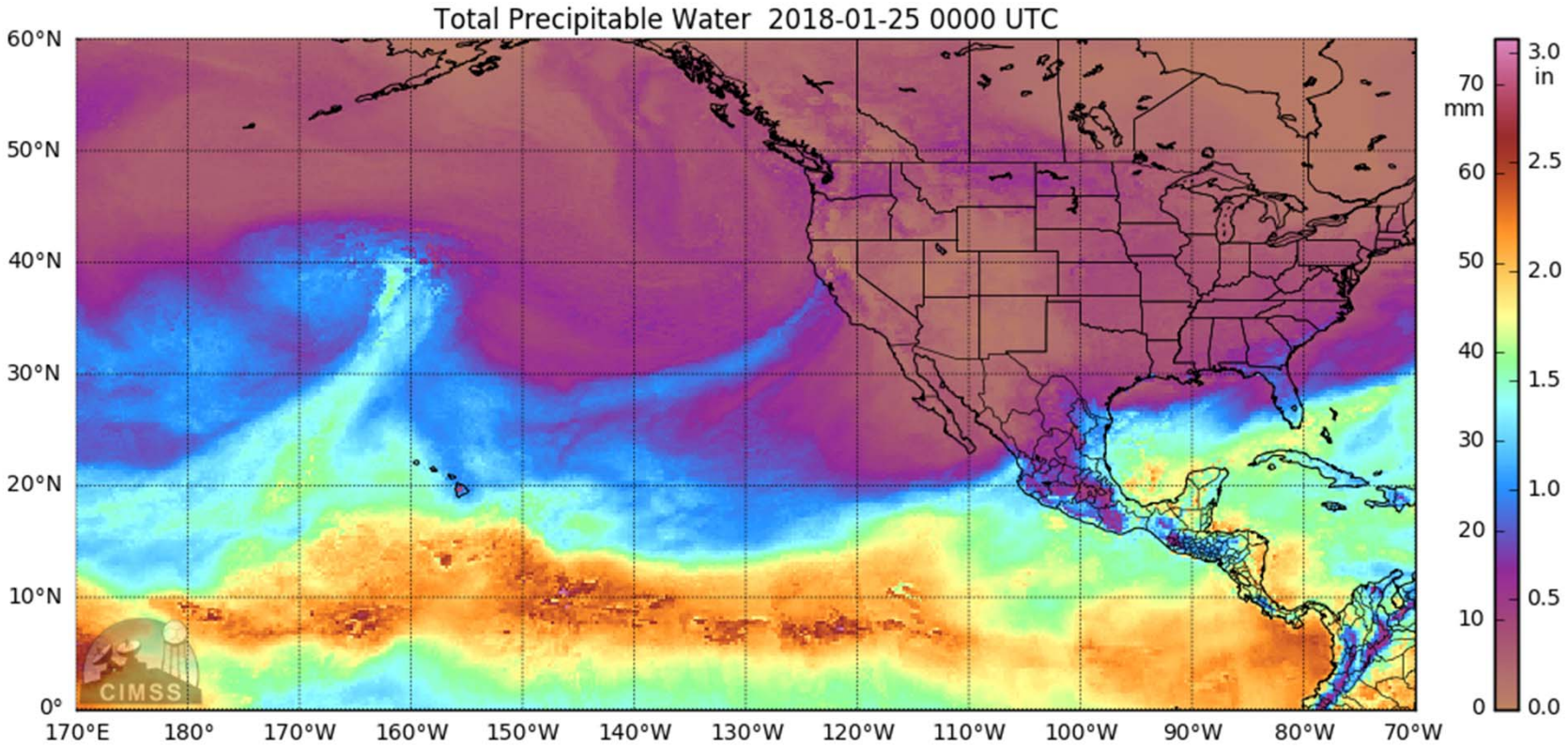

Atmospheric river event 27-29 January 2018

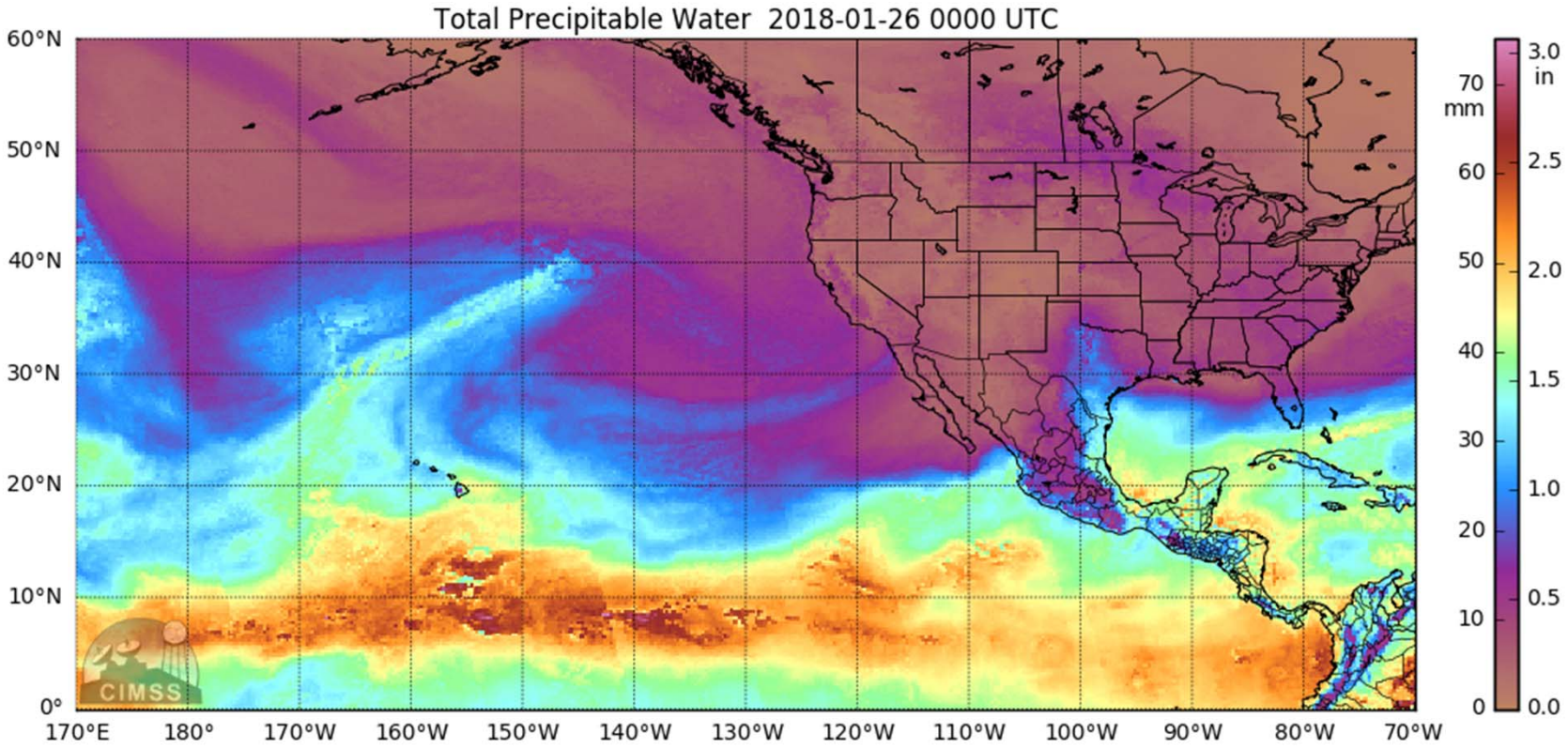

Atmospheric river event 27-29 January 2018

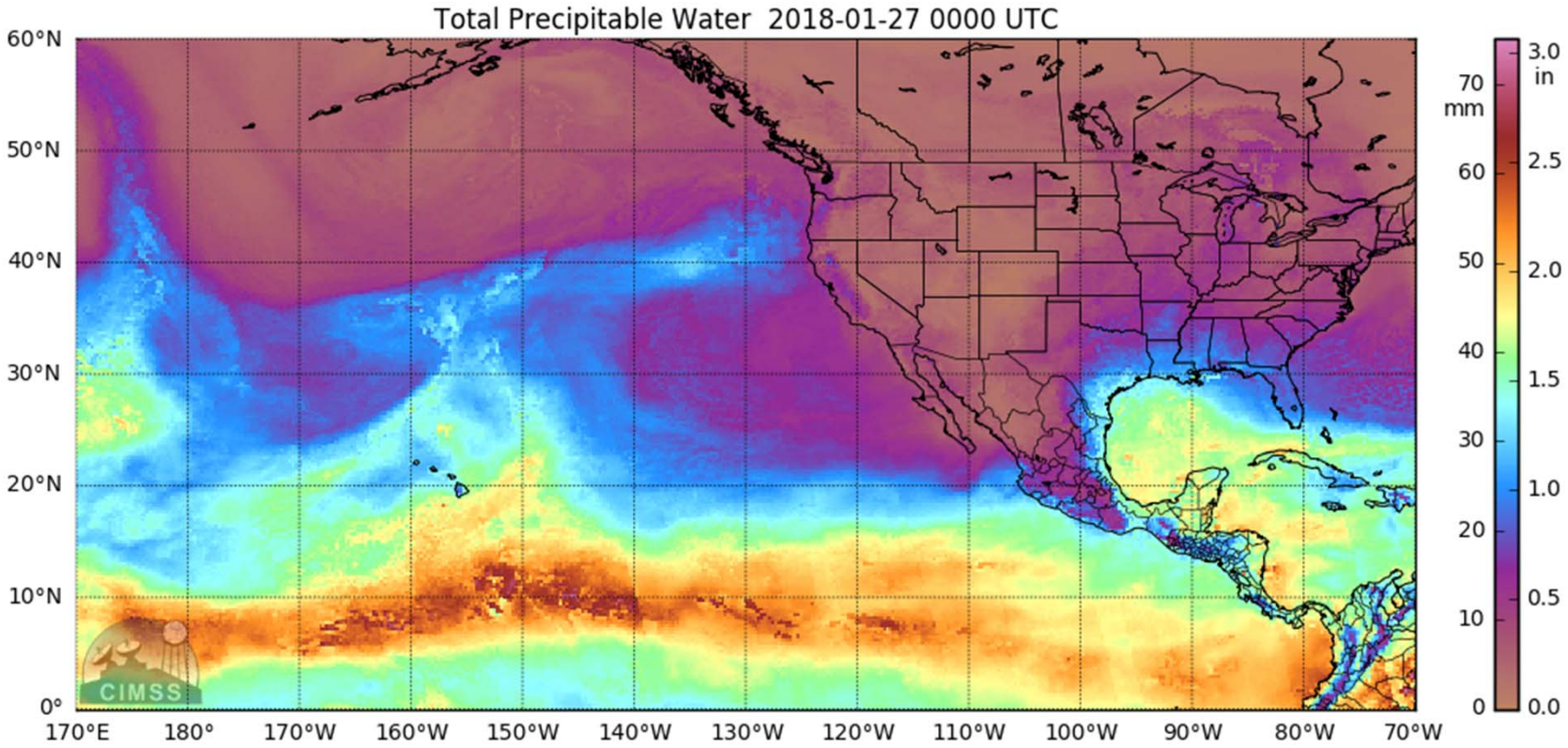

Atmospheric river event 27-29 January 2018

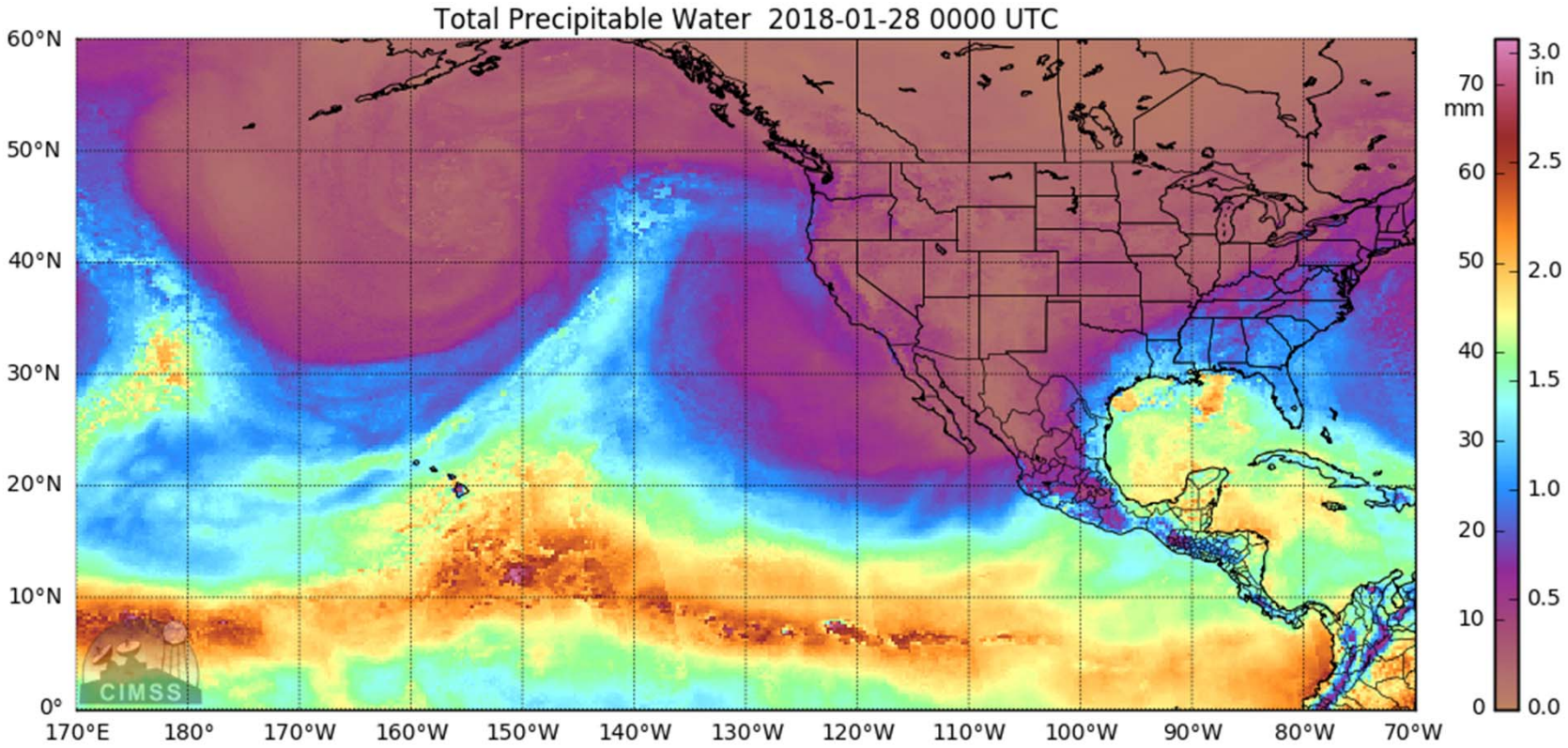

Atmospheric river event 27-29 January 2018

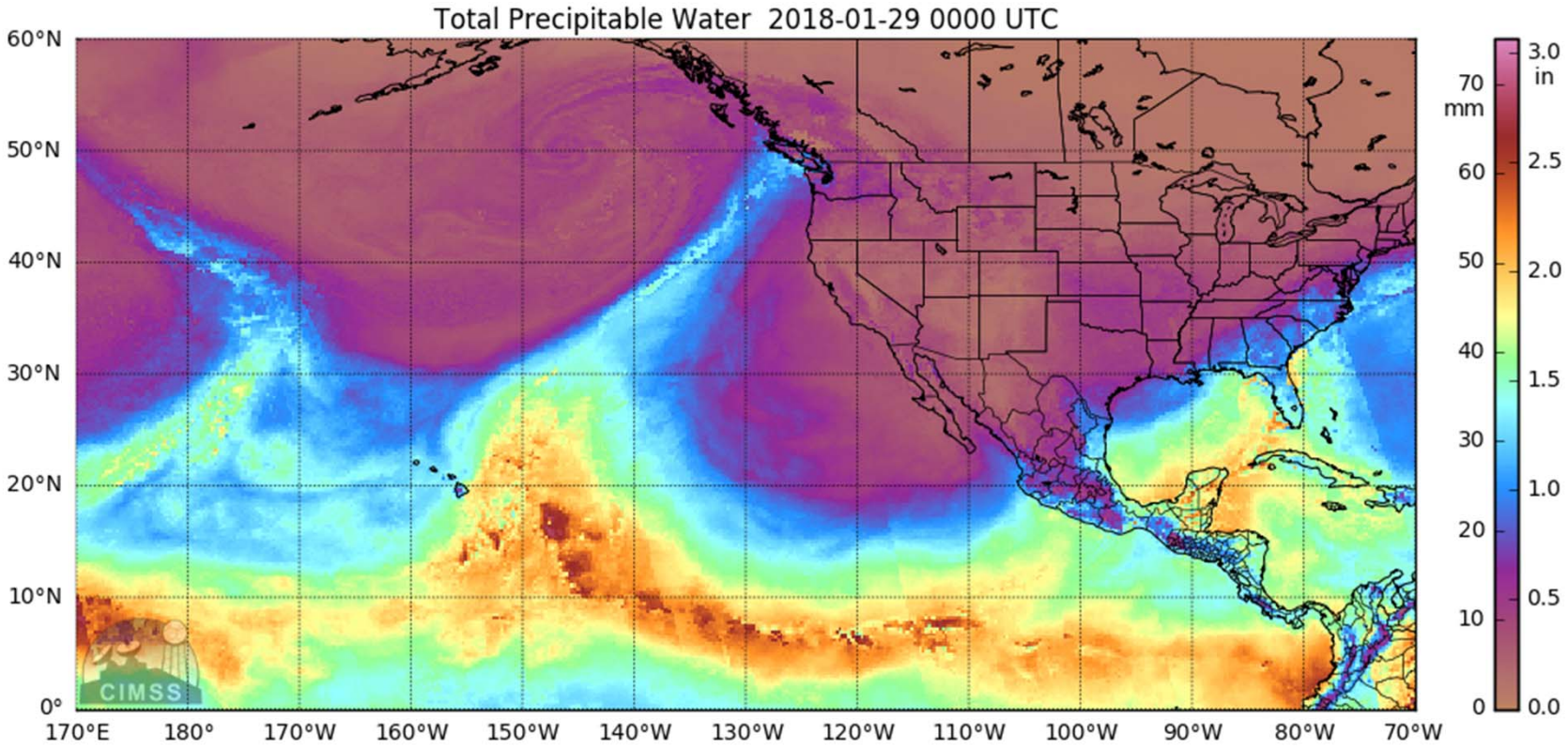

Center for Western Weather and Water Extremes

Atmospheric river reconnaissance field program:

supporting western storm predictions and water decisions

- F. Martin Ralph, PI
  - (UC San Diego/SIO/CW3E)
- Vijay Tallapragada Co-PI
  - (NOAA/NWS/NCEP)
- Jim Doyle
  - (Naval Research Laboratory)

UC San Diego | SCRIPPS INSTITUTION OF OCEANOGRAPHY

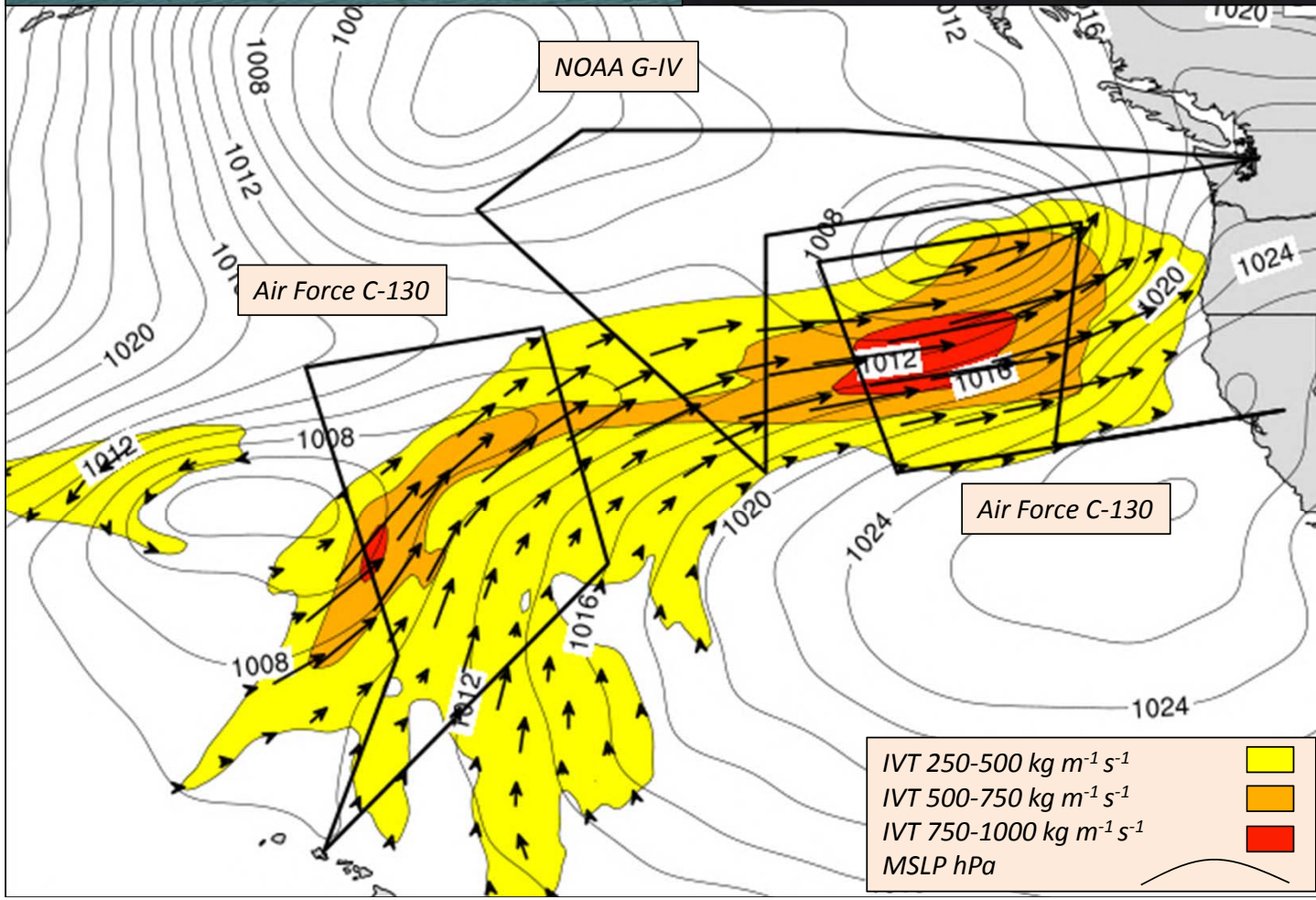

Research challenge: forecast sensitivity methods

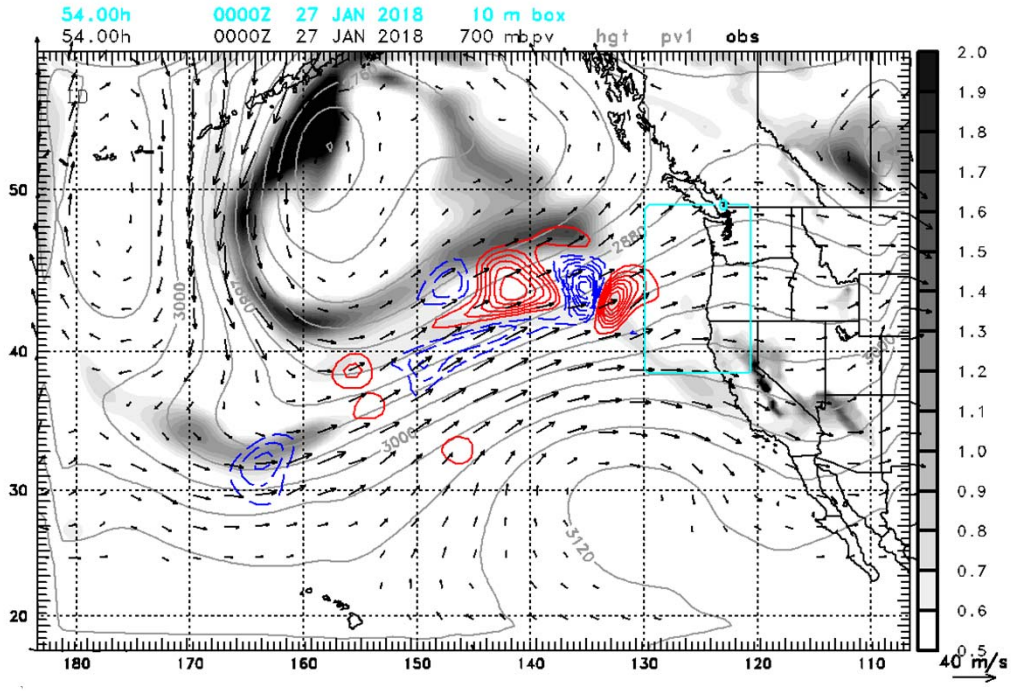

COAMPS Adjoint Sensitivity Valid at 00Z 27 January (54h)
700 hPa PV (gray)
700 hPa Heights (gray contour) and Winds (vectors)
700 hPa PV Sensitivity (blue/red)

See Reynolds et al., 2019, Adjoint Sensitivity of North Pacific Atmospheric River Forecasts, MWR

- The research challenge is finding a forecast sensitivity method that is effective in guiding the reconnaissance missions
- Example for 28 January 2018 event
- Left shows the adjoint sensitivity of the forecast 12h accumulated precipitation in the rectangle 24-36h after flight time to PV at 700 hPa at flight time 00Z 27 Jan
- A positive change in PV at the location shown in red will produce a negative change in precipitation.

Research challenge: forecast sensitivity methods

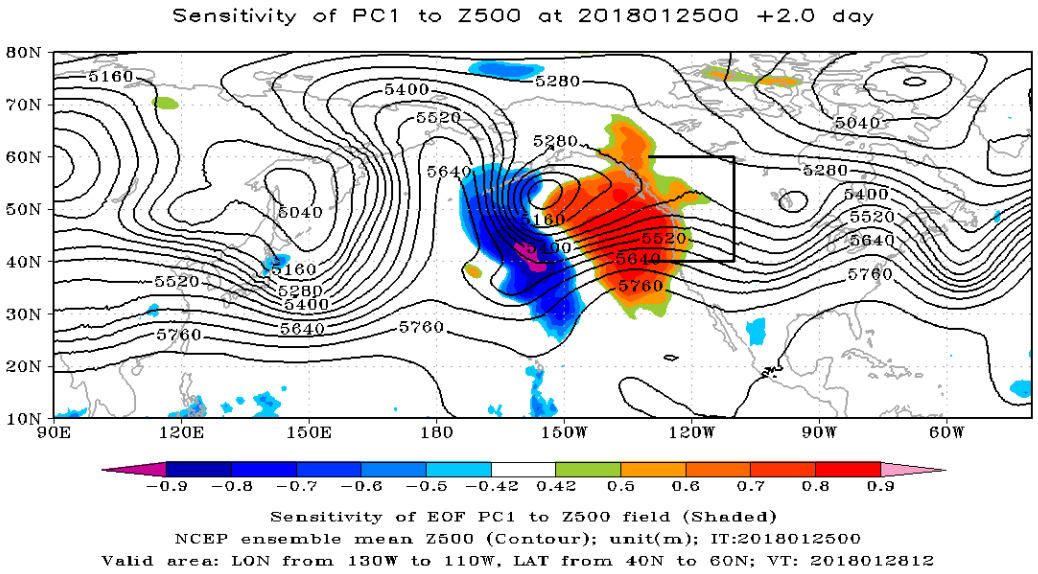

Zheng et al., 2013, Ensemble Sensitivity Tools for Assessing Extratropical Cyclone Intensity and Track Predictability, *Weather and Forecasting*

- Left shows the adjoint sensitivity of the 1st principle component of the variance of sea level pressure in the rectangle forecast for 12Z 28 January (24-36h after flight time) to Z500 at flight time 00Z 27 Jan
- A positive change in Z500 at the near the NOAA flight will produce a positive change in precipitation.
  - Forecast variable, observation variable?
  - Where to put the box?
  - Lead time? Changes every day
  - Confidence in scale of target sensitive area?

ARO data is complementary to dropsondes

- Dropsondes sample directly beneath the flight track (+ wind drift of sonde)
- Airborne Radio Occultation (ARO) samples to the side of aircraft, geometry is unaffected by winds
- High vertical resolution observations are made continuously, 25 per 7 hour flight, no expendable cost.
- The delay of the GNSS signal from a GNSS satellite below the horizon is observed through a Doppler shift in the carrier phase and refractive bending of the ray path.
- ARO provides a limb-sounding profile of refractivity, *N*, using the same technique as COSMIC satellites.
- Refractivity at tangent point is a function of pressure, temperature, water vapor pressure

$$N = (n-1)\cdot 10^6 = k_1 \frac{P}{T} + k_2' \frac{e}{T^2}$$

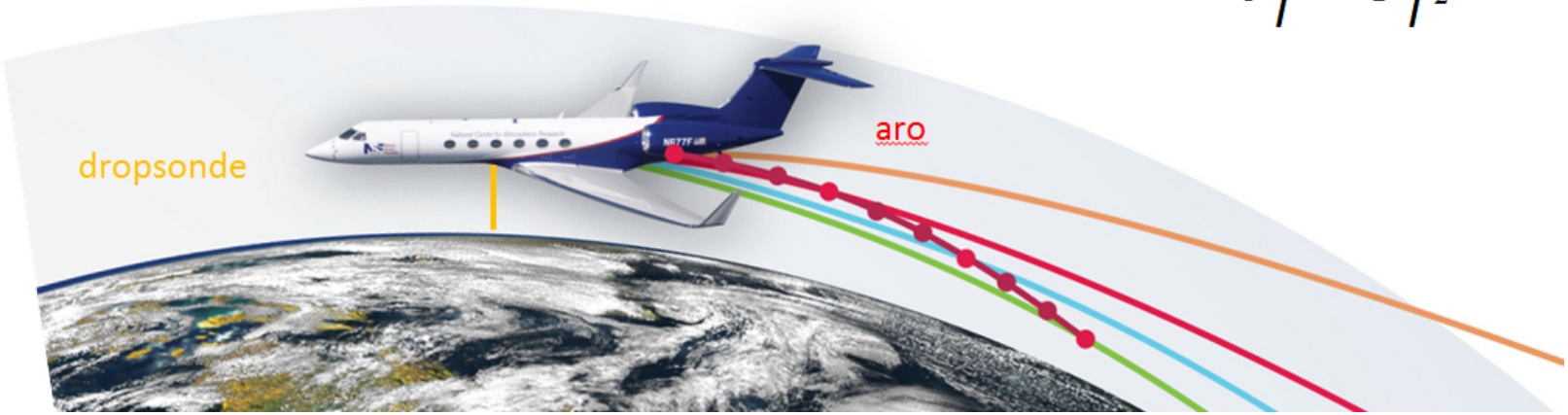

Vertical extent of ARO profiles

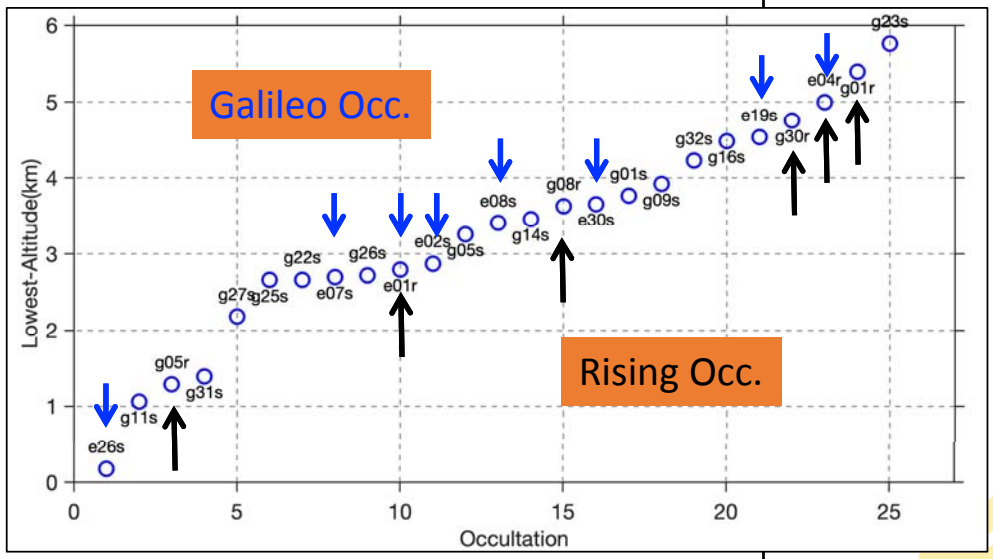

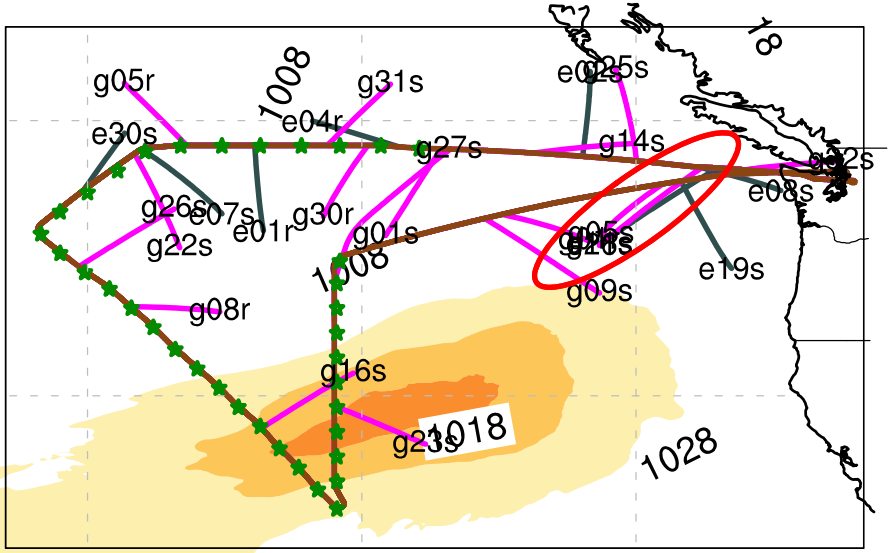

- ~8 hr flight.
- 17 GPS (14 Setting + 4 Rising).
- 8 Galileo (6 Setting +1 Rising).
- 11/25 occultations penetrate below 3 km.
- 18/25 occultations penetrate below 4 km.
- One Galileo occultation penetrates to the surface.
- Five rising occultations, one which penetrates to 2 km.
- EXCEPTIONALLY GOOD FOR SIMPLE CLOSED-LOOP RECEIVER HARDWARE.

ARO quali

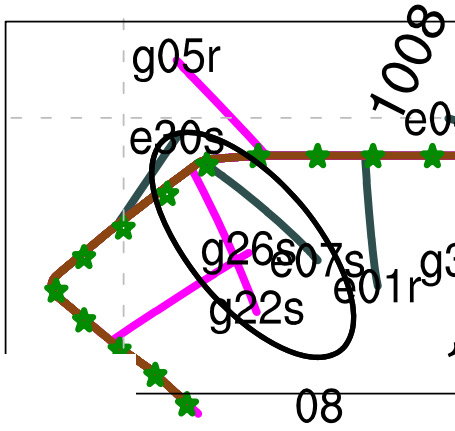
g05r
e20s
g26s
e07s
e01r
g22s
08

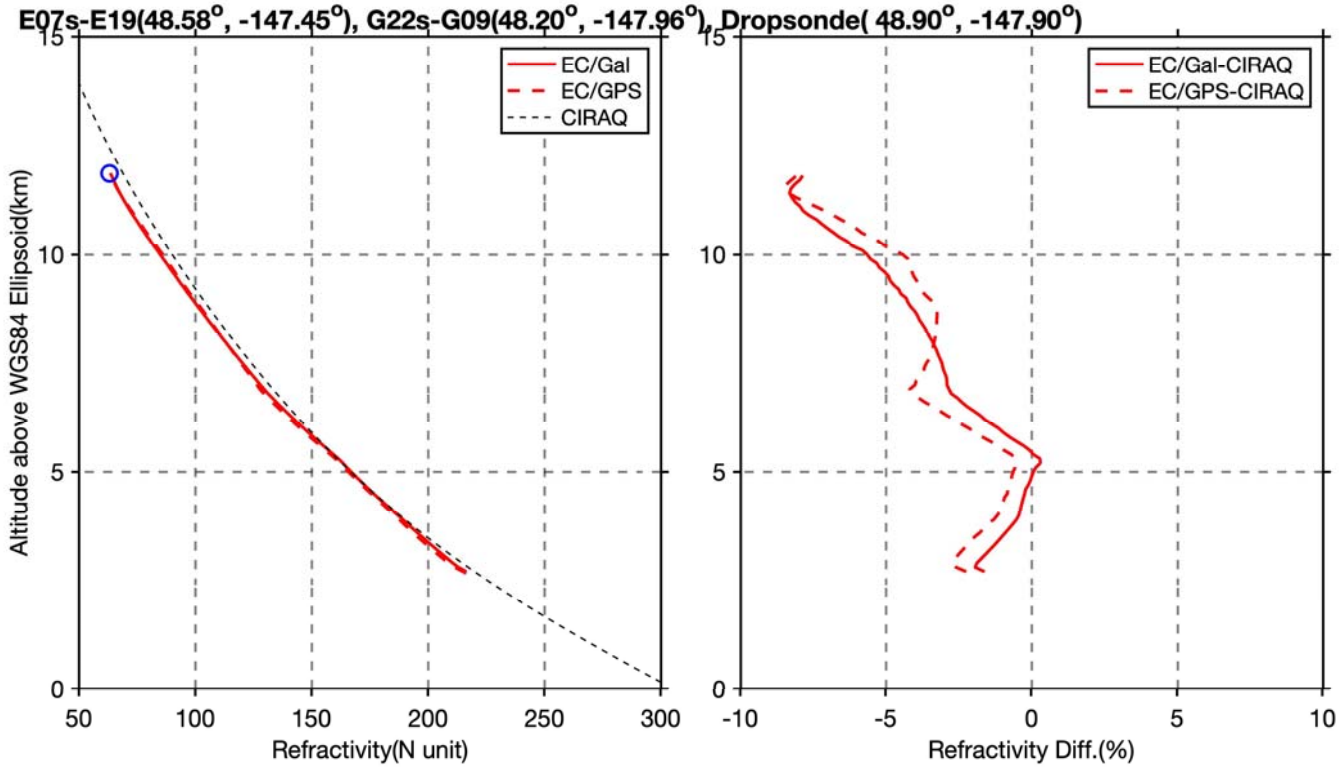
E07s-E19(48.58°, -147.45°), G22s-G09(48.20°, -147.96°), Dropsonde(48.90°, -147.90°)
EC/Gal
EC/GPS
CIRAQ
Altitude above WGS84 Ellipsoid(km)
Refractivity(N unit)
EC/Gal-CIRAQ
EC/GPS-CIRAQ
Refractivity Diff.(%)

ARO quali

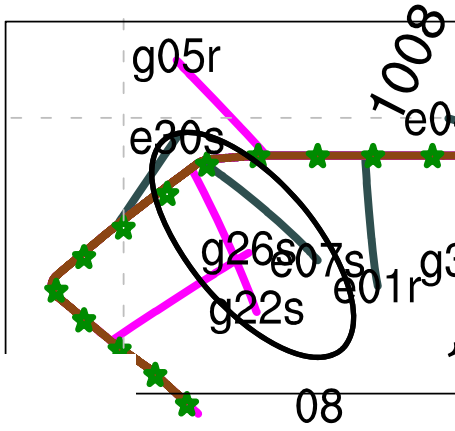
g05r
e20s
g26s
e07s
e01r
g22s
08

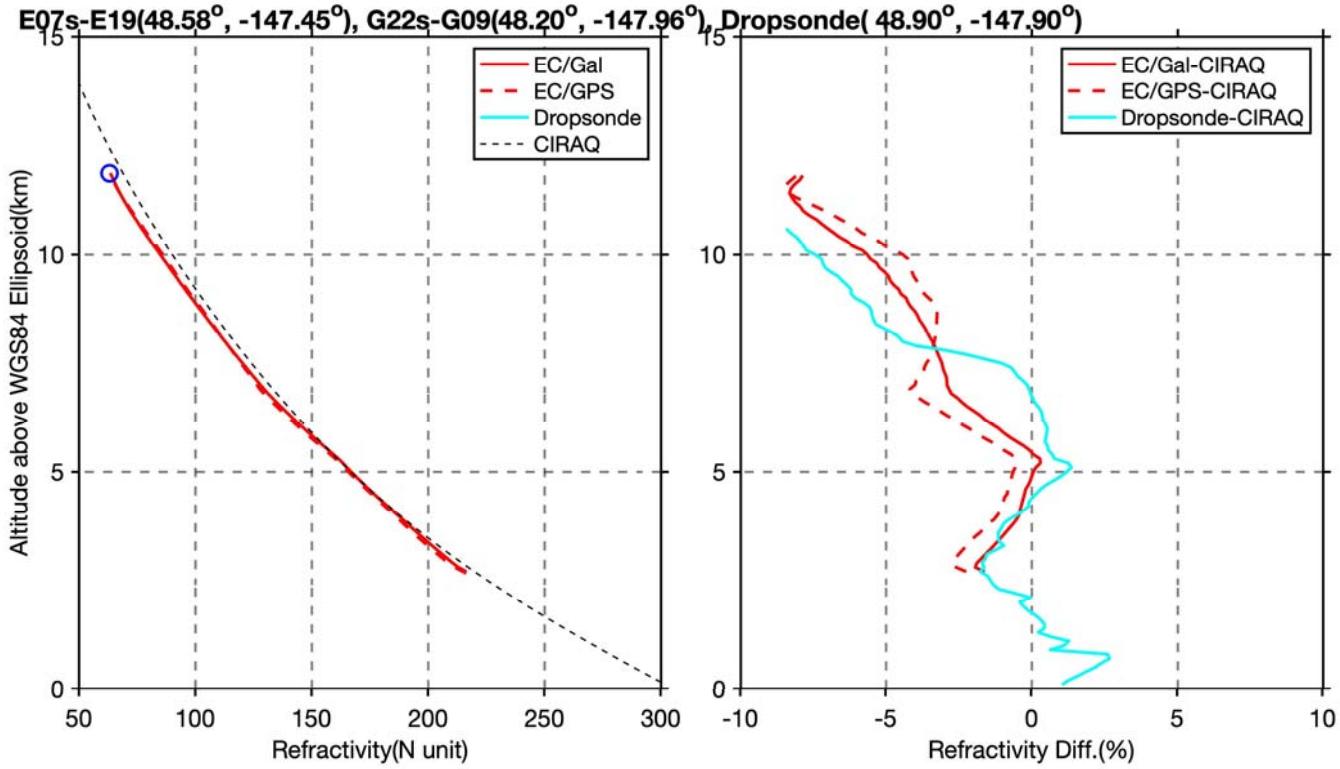
E07s-E19(48.58°, -147.45°), G22s-G09(48.20°, -147.96°), Dropsonde(48.90°, -147.90°)
EC/Gal
EC/GPS
Dropsonde
CIRAQ
Altitude above WGS84 Ellipsoid(km)
Refractivity(N unit)
EC/Gal-CIRAQ
EC/GPS-CIRAQ
Dropsonde-CIRAQ
Refractivity Diff.(%)

ARO quali

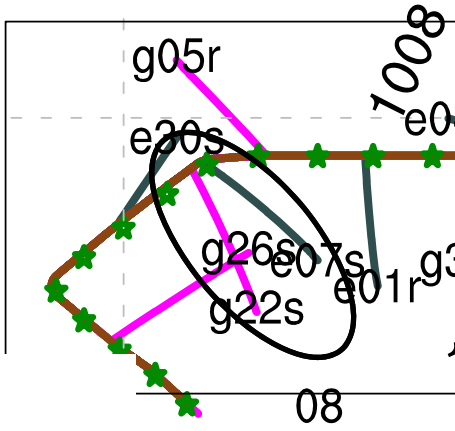
g05r
e30s
g26s
e07s
e01r
g22s
08

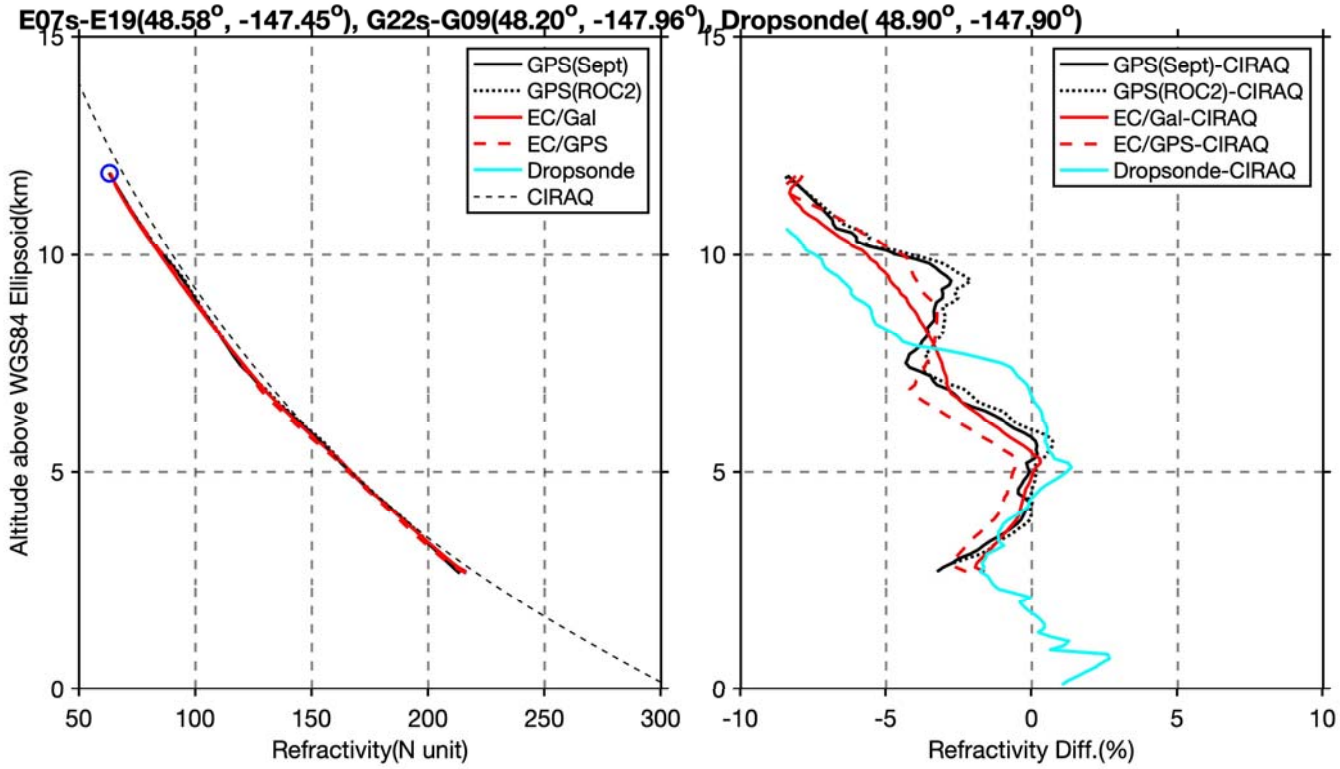
E07s-E19(48.58°, -147.45°), G22s-G09(48.20°, -147.96°), Dropsonde(48.90°, -147.90°)
GPS(Sept)
GPS(ROC2)
EC/Gal
EC/GPS
Dropsonde
CIRAQ
Altitude above WGS84 Ellipsoid(km)
Refractivity(N unit)
GPS(Sept)-CIRAQ
GPS(ROC2)-CIRAQ
EC/Gal-CIRAQ
EC/GPS-CIRAQ
Dropsonde-CIRAQ
Refractivity Diff.(%)

ARO quali

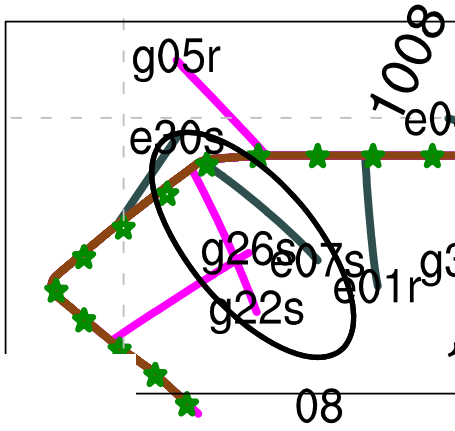
g05r
e30s
g26s
e07s
e01r
g22s
08

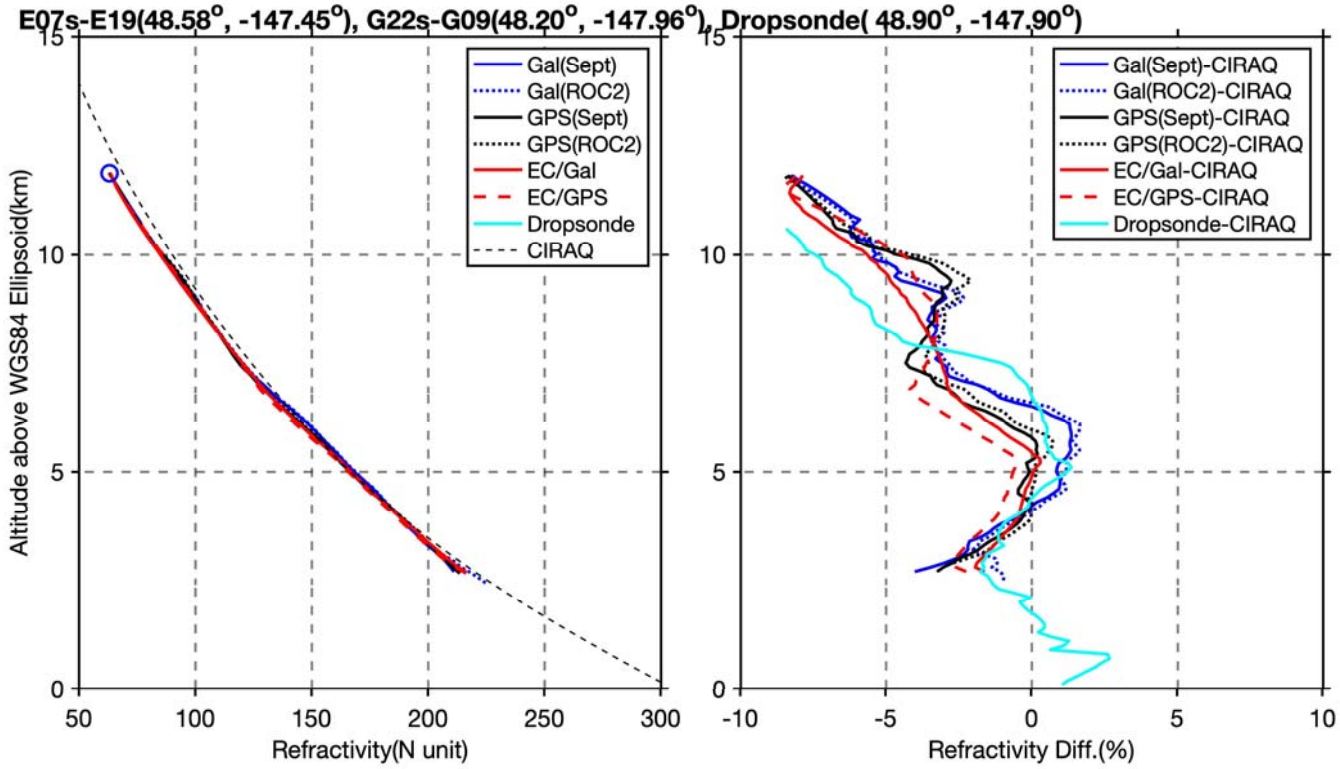
E07s-E19(48.58°, -147.45°), G22s-G09(48.20°, -147.96°), Dropsonde(48.90°, -147.90°)
Altitude above WGS84 Ellipsoid(km)
Refractivity(N unit)
Refractivity Diff.(%)
Gal(Sept)
Gal(ROC2)
GPS(Sept)
GPS(ROC2)
EC/Gal
EC/GPS
Dropsonde
CIRAQ
Gal(Sept)-CIRAQ
Gal(ROC2)-CIRAQ
GPS(Sept)-CIRAQ
GPS(ROC2)-CIRAQ
EC/Gal-CIRAQ
EC/GPS-CIRAQ
Dropsonde-CIRAQ

ARO quality evaluatio

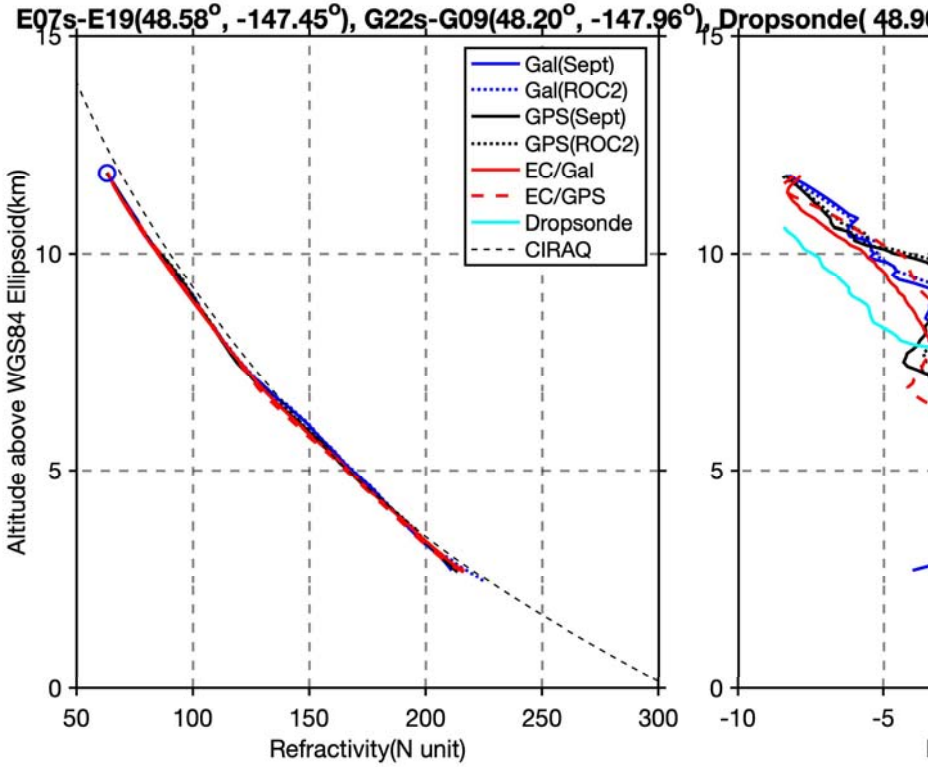

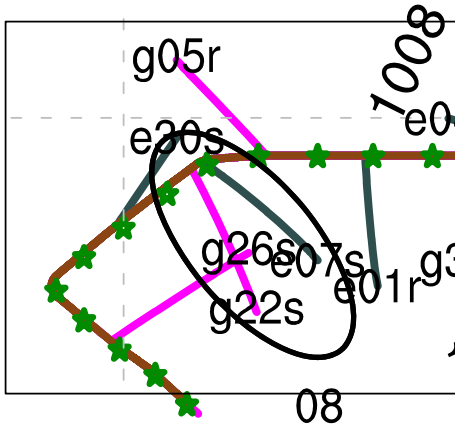

ARO quality evaluatio

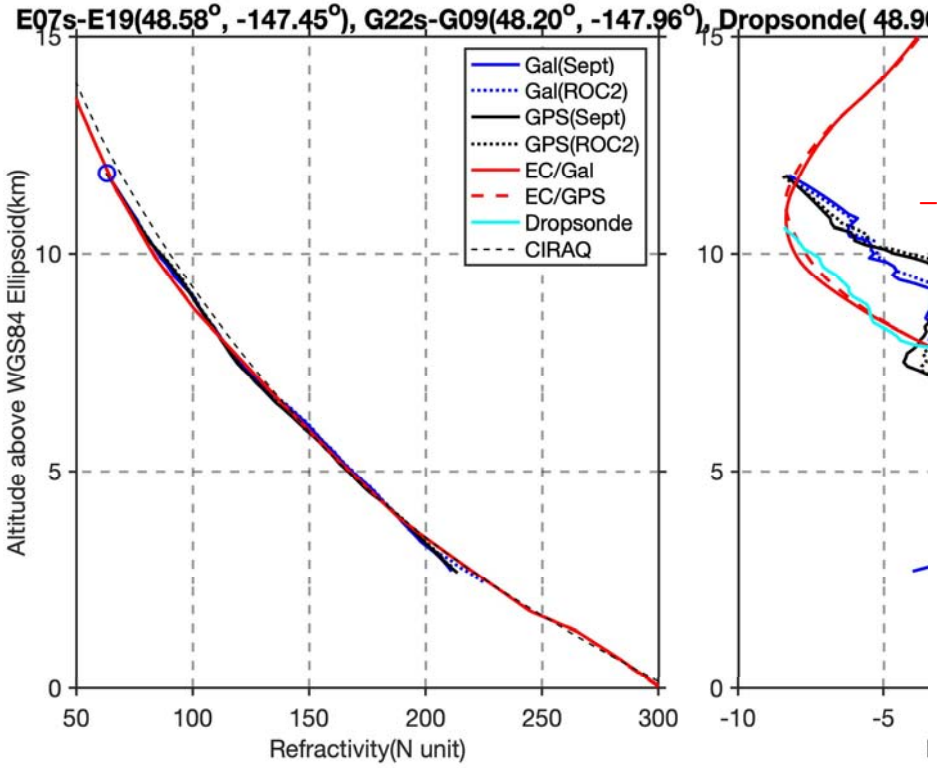

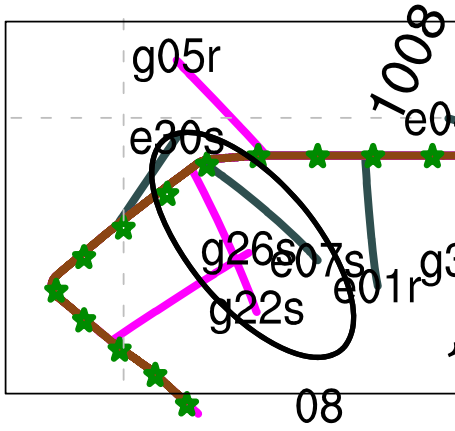

EC at dropsonde location

GPS / Galileo SNR Comparison

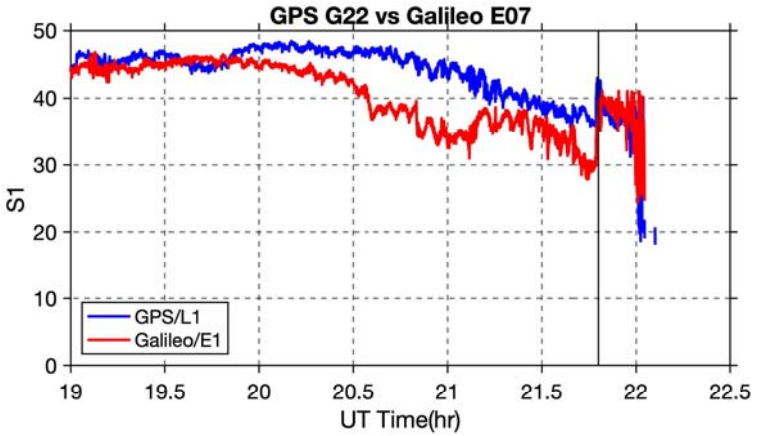

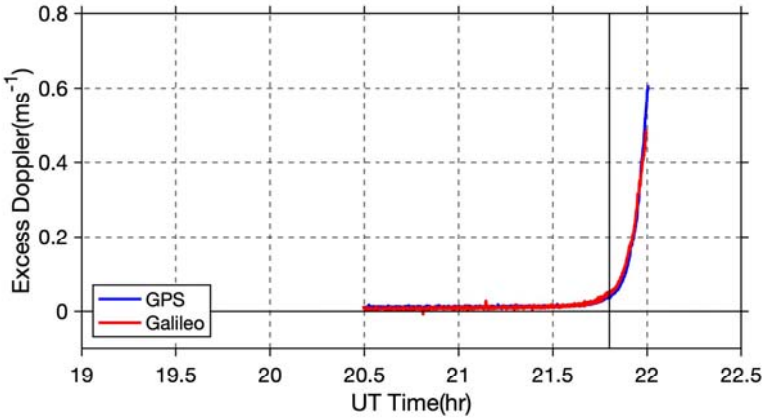

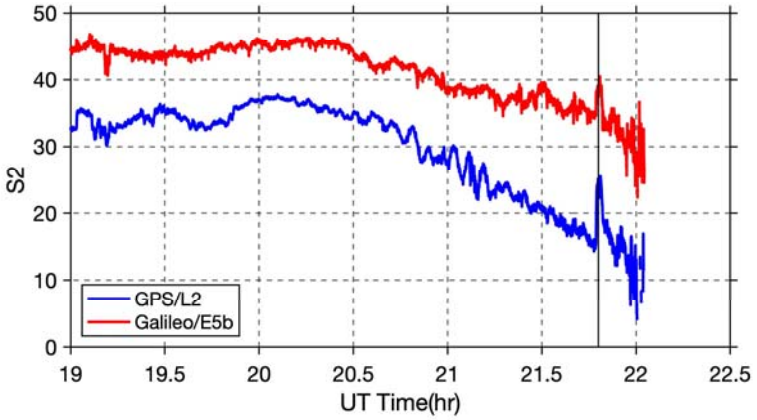

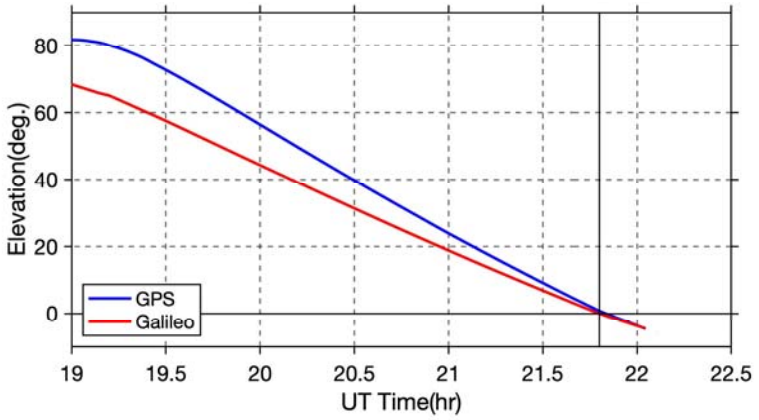

WRF DROPS Temperature@ 7 km

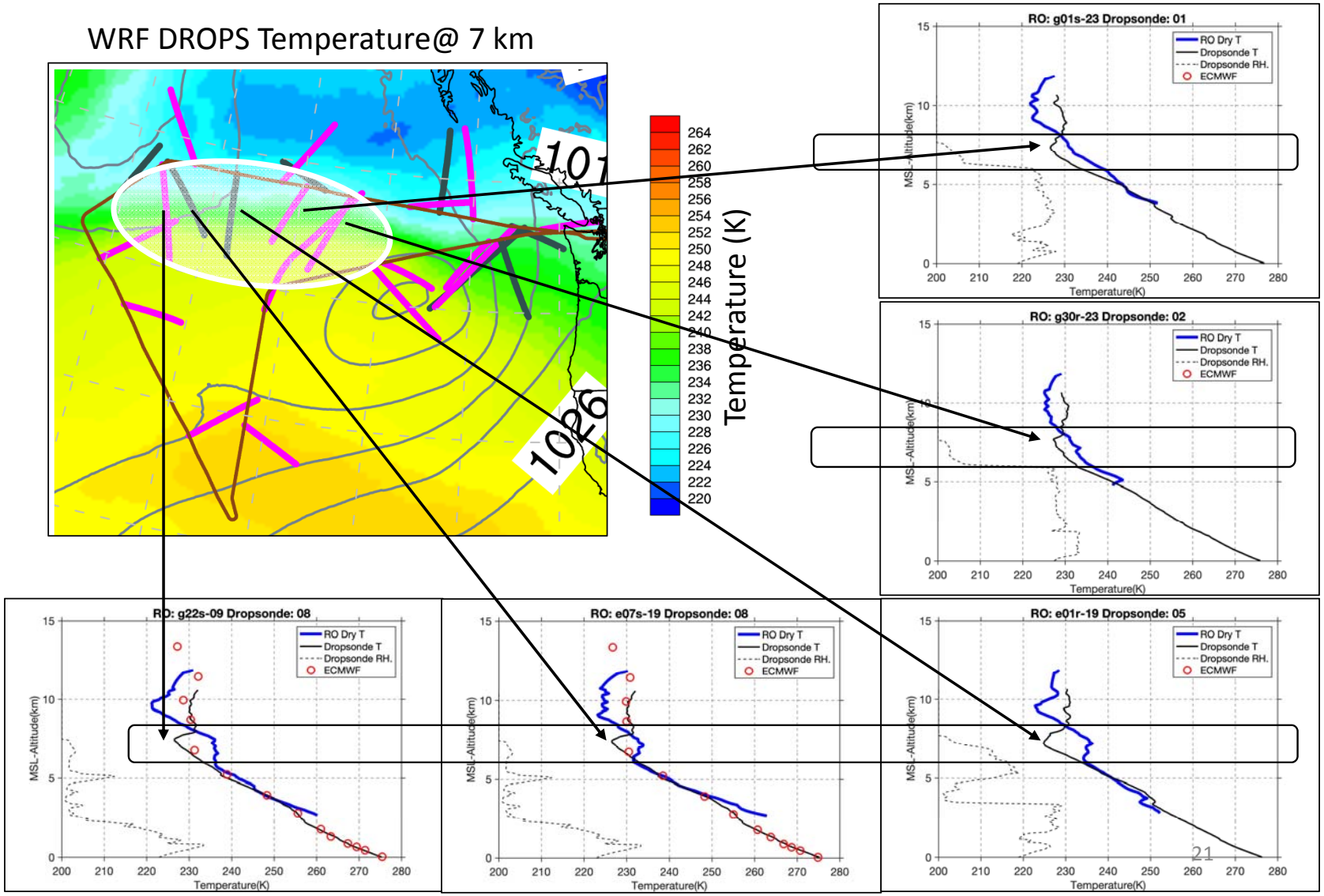

- Systematic fluctuations in temperature over the range from 6-11 km altitude correspond to strong temperature gradient in hi-res WRF model run that assimilates dropsondes.

WRF DROPS Temperature@ 10.5 km

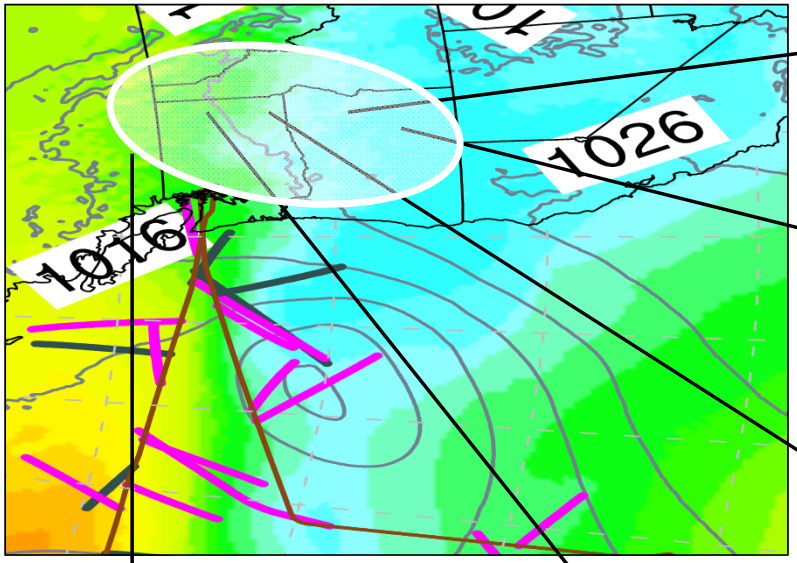

Temperature (K)

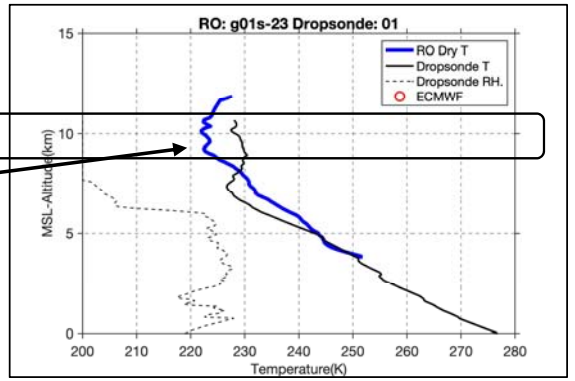

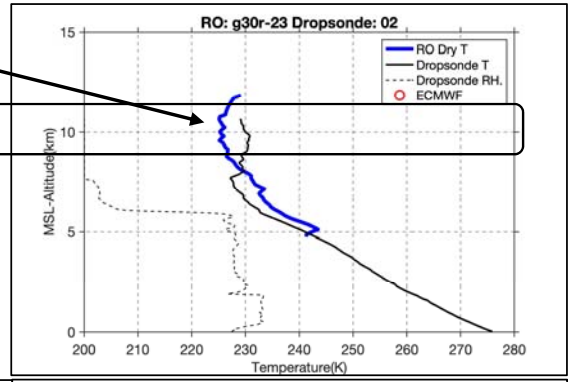

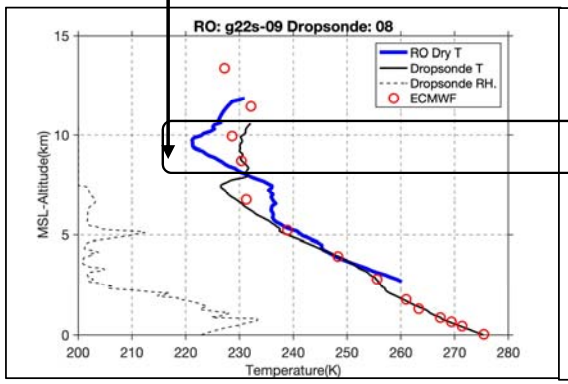

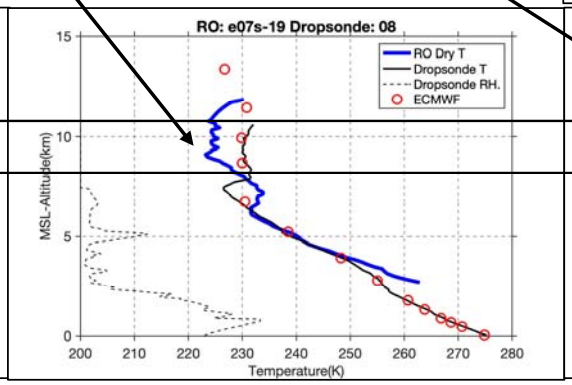

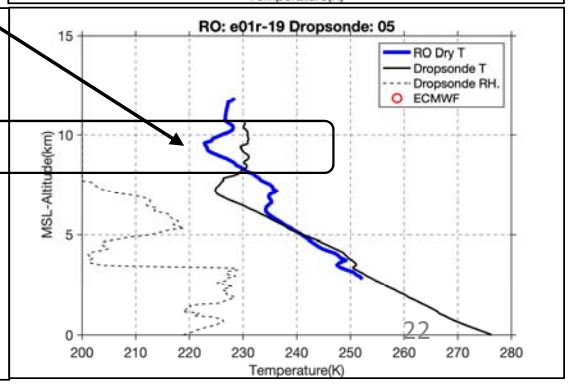

- Systematic fluctuations in temperature over the range from 6-11 km altitude are opposite sign at 1.5 km where temperature gradient is reversed. Possible wave pattern.

ARO data assimilation experiments

Atmospheric River offshore													Landfall												NonAR cyclogenesis											
													Landfall Oregon																							
																													Landfall and heavy precipitation Vancouver Is.									
Experiments (no cycling)																																				
26 Jan								27 Jan										28 Jan										29 Jan									30 Jan				
0:00	3:00	6:00	9:00	12:00	15:00	18:00	21:00	0:00	3:00	6:00	9:00	12:00	15:00	18:00	21:00	0:00	3:00	6:00	9:00	12:00	15:00	18:00	21:00	0:00	3:00	6:00	9:00	12:00	15:00	18:00	21:00	0:00	3:00	6:00	9:00	12:00
						Start Cold Run																														
						GEFS ensemble as IC/BC run forward for 4 days																																
						B/C		B/C		B/C		B/C		B/C		B/C		B/C		B/C		B/C		B/C		B/C		B/C		B/C		B/C		B/C		B/C
								3DVar data assimilation 1 cycle on outer domain D01																														
								Free forecast for 4 days using updated analysis and B/C on nested grid with two domains D01 and D02																														
Observations																																				
G-4 Flights						RF01 2000 - 0200 Z																																
						ARO Observations available for DA = 25 profiles																																
C-130 HI						RF01 2000 - 0300 Z																								RF02 2000 - 0300 Z								
C-130 CA						RF01 1900 - 0200 Z																								RF02 1900 - 0200 Z								
						8	49	30	=	87 dropsondes total for DA																				8	25	18	=	51 dropsondes available for verification				

Config 07.01 (GEFS forcing with Ensembles)		
	14.7X	
Description	two domains	
Forecast model	WRF-ARW V4.1	
DA System	WRFDA V4.1	
DA technique	3DVAR **No Cycling ASCII prepbufr**	
Initial/Bdry Conditi	GEFS Operational Forecast (from HAS 1.0 deg)	
# of ensembles	0 i.e. just the cntrl member (ens00)	
Domains	D01	D02
Assmilation	yes	no
Resolution	27 km	9 km
Mesh size	355 x 300	799 x 661
Nest feedbak	two way	two way
Model levels	48	
Model top	10 hPa	

Microphysics	Thompson (Double-Moment)	
Cumulus	Grell-Freitas	Grell-Freitas
PBL	YSU scheme	
Land Surface	Unified Noah land-surface model	
Longwave	RRTMG	
Shortwave	RRTMG	
Background Error	NMC method (24-12 hr fcsts)	
	15 Jan - 15 Feb 2018	
	intitalized at 00 & 12 UTC	
BE System	WRFDA GENBE V1.0	
	BE Covariance 5	

SOUND_ONLY	ARO_G_ONLY	ARO_GE	GPSRO	DROP	DROP_ARO
14.12	14.13	14.14	14.15	14.72	14.77
radiosonde + drops	ARO GPS	ARO GPS + Galileo	GNSSRO bufr	GTS + radiosonde + drops	GTS + radiosonde + drops + ARO

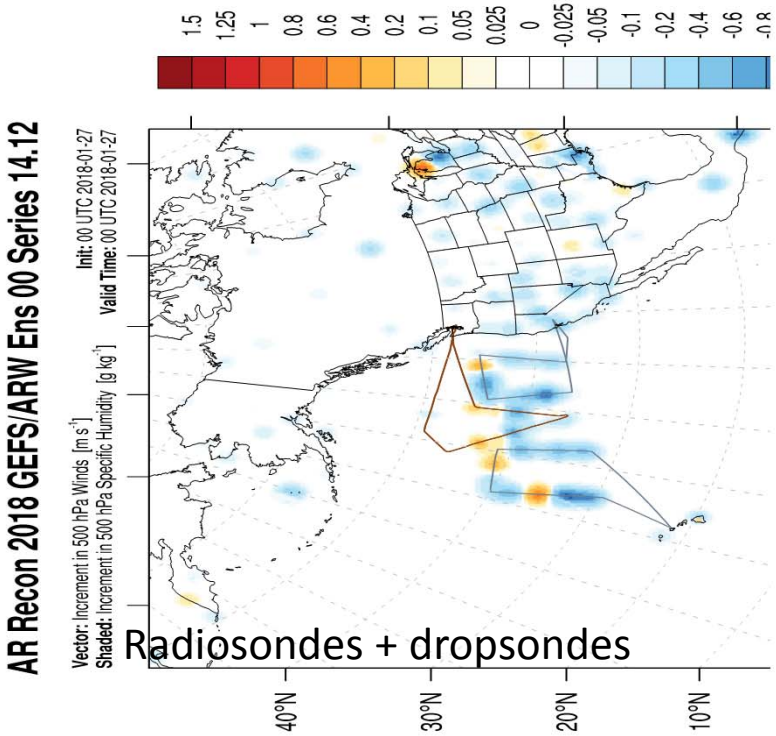

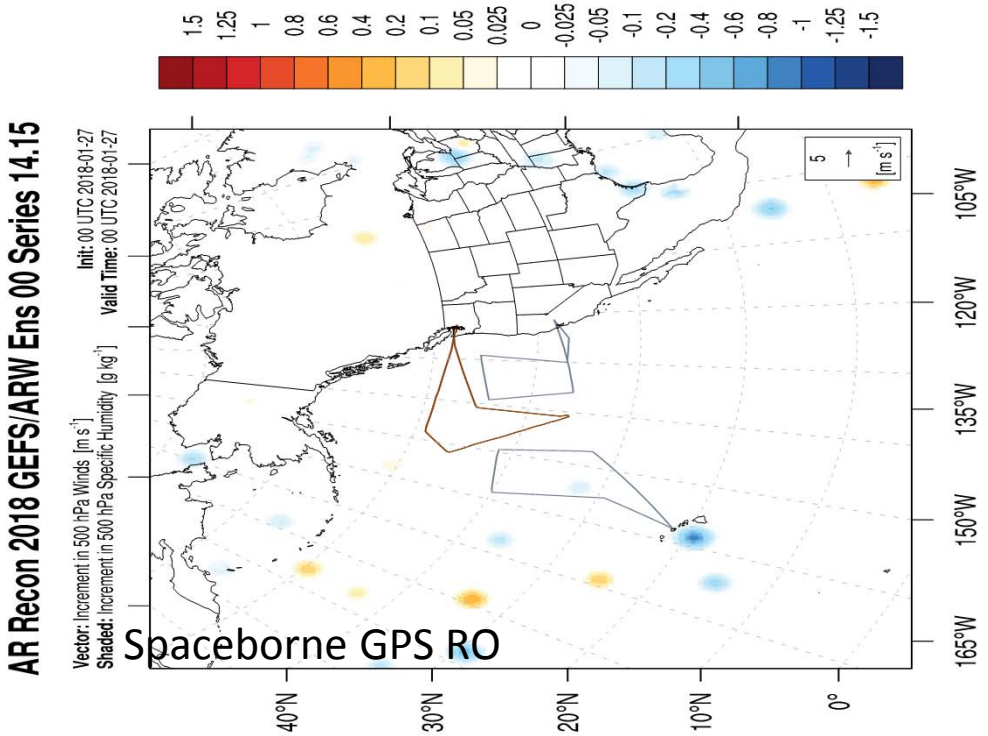

AR Recon 2018 GEFS/ARW Ens 00 Series 14.13

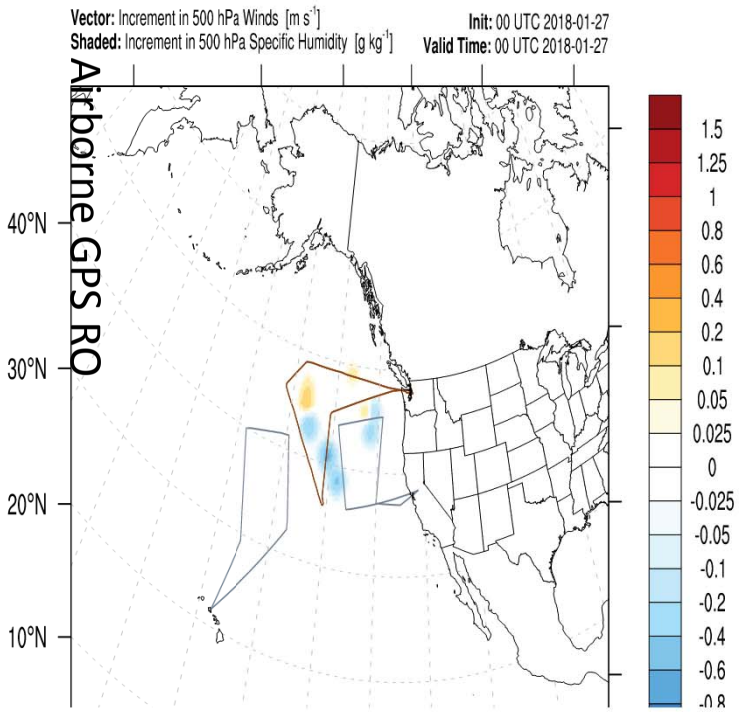

Airborne GPS RO

AR Recon 2018 GEFS/ARW Ens 00 Series 14.14

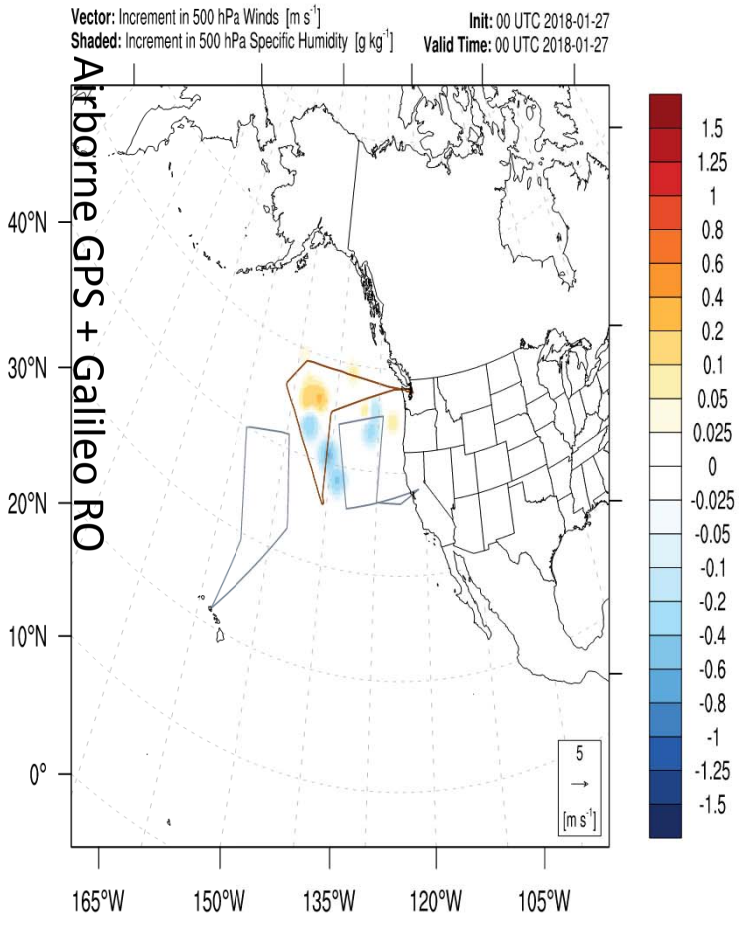

Airborne GPS + Galileo RO

AR Recon 2018 GEFS/ARW Ens 00 Series 14.72

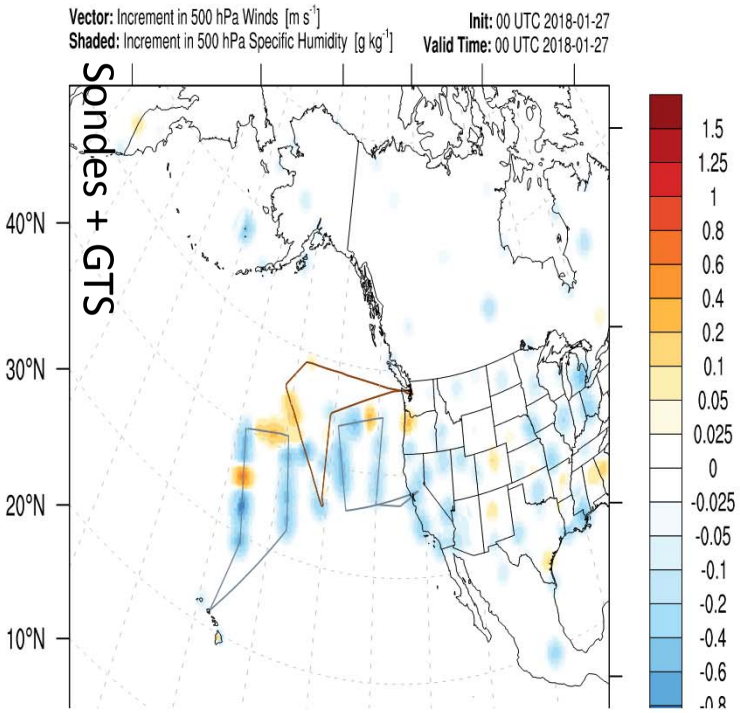

AR Recon 2018 GEFS/ARW Ens 00 Series 14.77

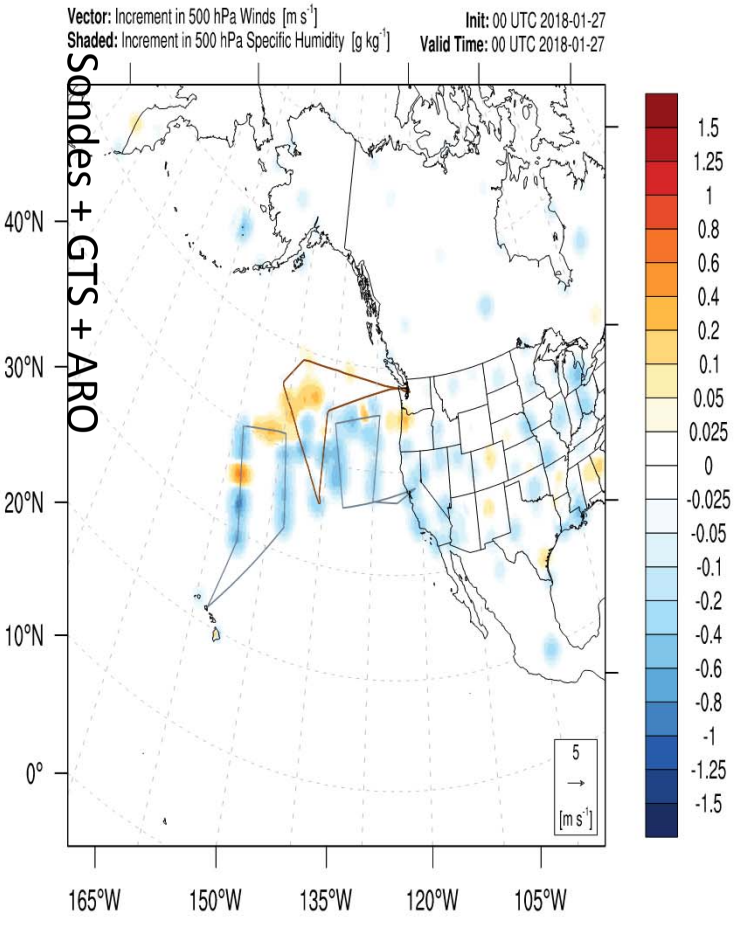

Influence on 12 hour forecast

Difference in Spec. Hum.

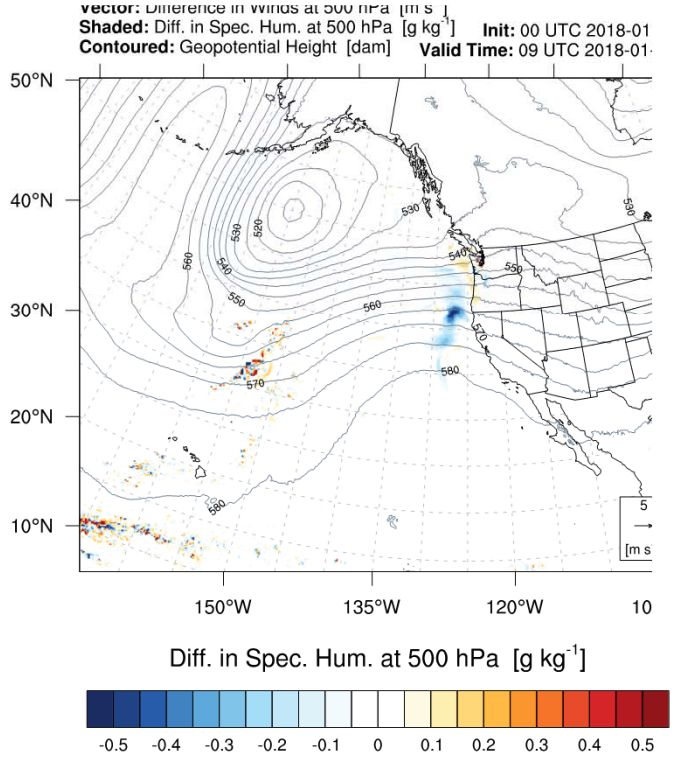

Difference in precipitation

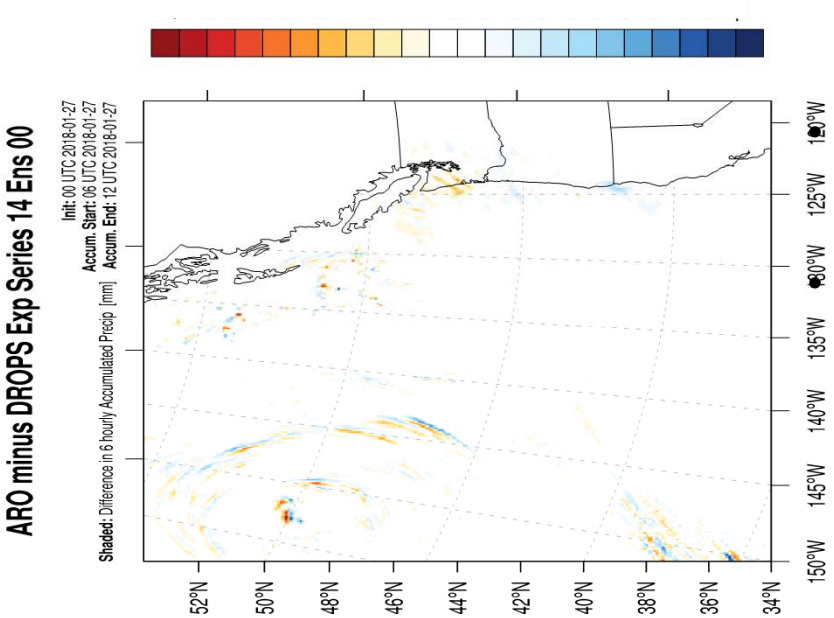

- ARO had an impact on the initial moisture fields that propagated downstream and affected precipitation at landfall.
- In this case, the precipitation was minor so the overall impact was minor.
- Now that we are up and running, we want to design better experiments to investigate and define criteria based on the sensitivity calculations
  - Which events to fly
  - Where to sample
  - Which day to fly

Investigation of SPIRE data

- Heavy storm swept through Southern California on 5-6 Dec 2018, and brought heavy rainfall to the region.
  - 3-day precip totals > 6.4 cm
  - Some coastal regions > 5 cm/6hr
  - Post-wildfire debris flows
  - Such events bring 20% of annual rainfall
  - 3 and 1 day forecast underestimated rainfall by up to 2.5 cm
- 37 profiles in model domain
- 4 within AR, 1 near integrated vapor transport (IVT) maximum
- Most profiles at ~ 07:00 to 09:00 UTC
- Gap of ~1000 km from IVT max to coast

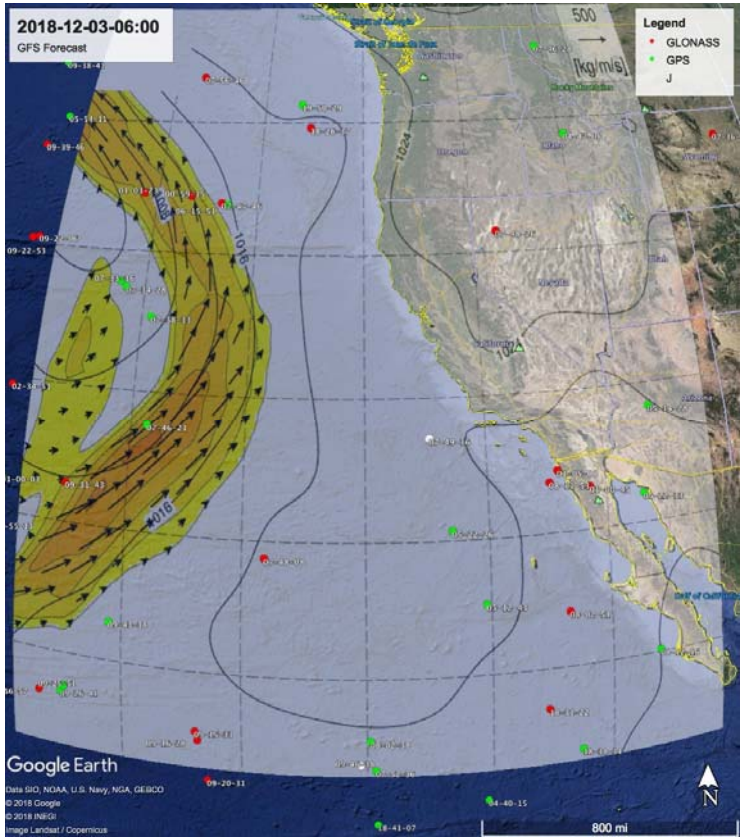

Investigation of SPIRE data

- Heavy storm swept through Southern California on 5-6 Dec 2018, and brought heavy rainfall to the region.
  - 3-day precip totals > 6.4 cm
  - Some coastal regions > 5 cm/6hr
  - Post-wildfire debris flows
  - Such events bring 20% of annual rainfall
  - 3 and 1 day forecast underestimated rainfall by up to 2.5 cm
- 37 profiles in model domain
- 4 within AR, 1 near integrated vapor transport (IVT) maximum
- Most profiles at ~ 07:00 to 09:00 UTC
- Gap of ~1000 km from IVT max to coast

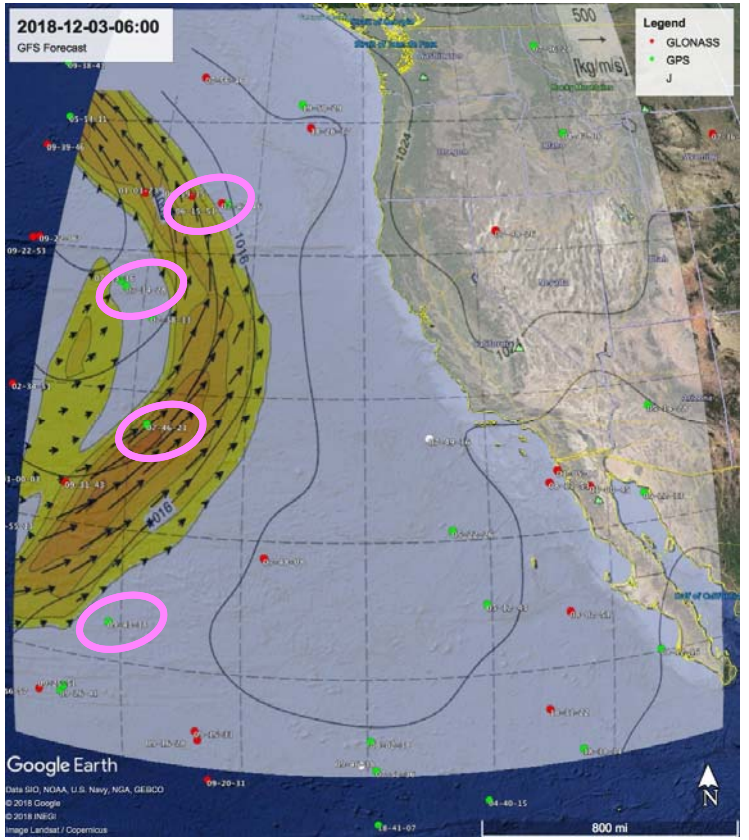

Investigation of SPIRE data

- Preliminary comparison of observed N to ECMWF Reanalysis 5 (ERA5)
- Good north to south transect of profiles

$$N = (n-1)\cdot 10^6 = k_1 \frac{P}{T} + k_2' \frac{e}{T^2}$$

- Some concerns with consistency from preliminary analysis

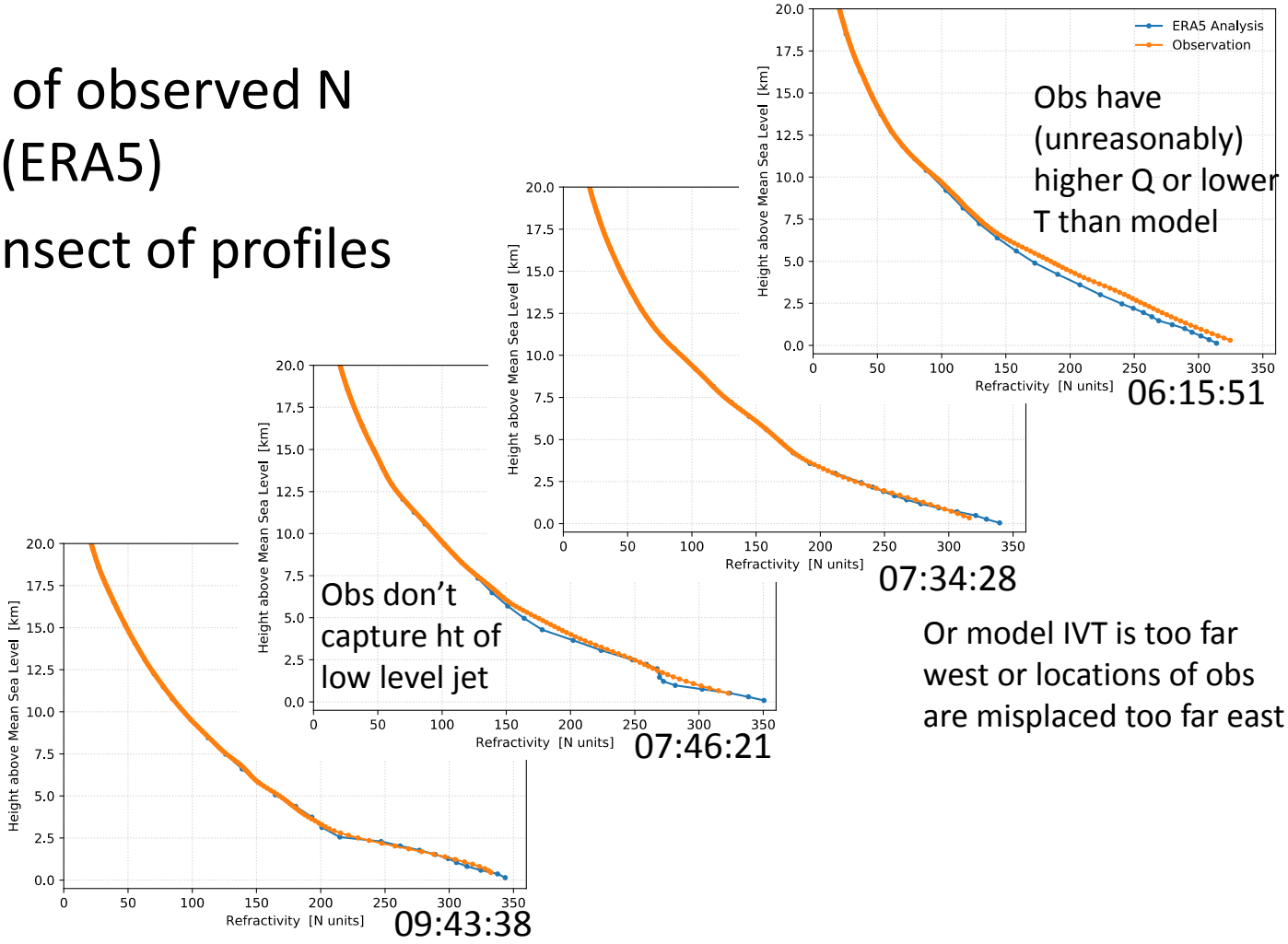

Or model IVT is too far west or locations of obs are misplaced too far east

Initial Assessment

- Spatial and temporal data distribution that was provided is not good for accomplishing the science objectives
- Metadata is nonexistent for data release 2
- Overall 64326 profiles in 75 days = ~1/ 7^{o}x7^{o} box / day
- on 2018-12-03: ~4 / 5^{o}x5^{o} box / day = 0.2 / 1^{o}x1^{o} box / day
  - Target for atmospheric rivers is 4 / 1^{o}x1^{o} box / day in area of interest
- Major concern is sampling the moist low-level jet
  - 22 of 37 profiles in domain extend below 1 km (relatively good)
  - 3 bad profiles – extend below 0 but flagged with badness

Metadata requirements – User perspective

- As mesoscale users we WOULD REALLY LIKE TO SEE the following:
- Online searchable database with user selected search parameters
- Online graphical spatial selection capability
- User friendly (ie efficient) download capability (selecting multi files)
- Quick looks
- API for searching and downloading data
- Complete archive of historical data
- Online documentation of all parameters for new data assimilation users
- Online documentation of data releases/updates w/release notes
- Online documentation of SATELLITE SPECIFIC updates
- User support email address and phone number

Conclusions and Discussion

- ARO data provide a good way to investigate the accuracy, variability, and repeatability of refractivity profiling in the 3D heterogeneous lower troposphere that is not possible with sparsely sampled spaceborne RO. Experiments provide a focus on critical events of interest.
- Initial ARO data assimilation shows consistent and complimentary analysis increments compared to dropsondes during research flights. => They provide similar impact.
- We have done some experiments with GSI and the nonlocal excess phase operator, and see great advantages in coordinating efforts with ROM-SAF (ROPP) and JCSDA (JEDI) for supporting and maintaining assimilation capabilities.
- For the mesoscale, time distribution of profiles is critical
- NOAA AOC has committed to hosting ARO on the G-IV for the next 5 years, and Air Force is also open to hosting again on their C-130s.
- We are ssssloowwwwlly ramping up to a project using commercial aircraft.

New and Future Science

Polarimetric ARO Sensitivity

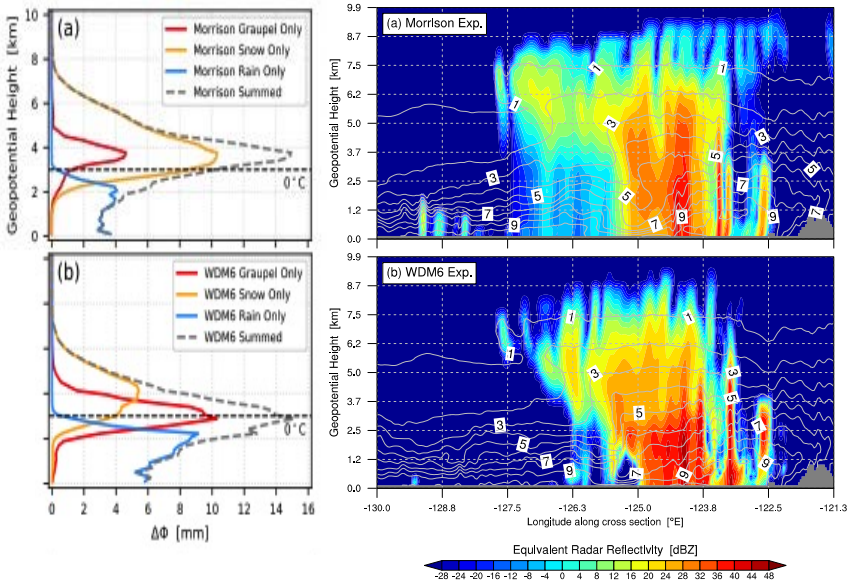

Murphy, Haase, Padulles, Chen, Morris (2019), The Potential for Discriminating Microphysical Processes in Numerical Weather Forecasts using Airborne Polarimetric Radio Occultations, *Remote Sensing Special Issue "Radar Polarimetry—Applications in Remote Sensing of the Atmosphere"*, *Submitted*.

Strateole-2 Stratospheric Balloon ROC

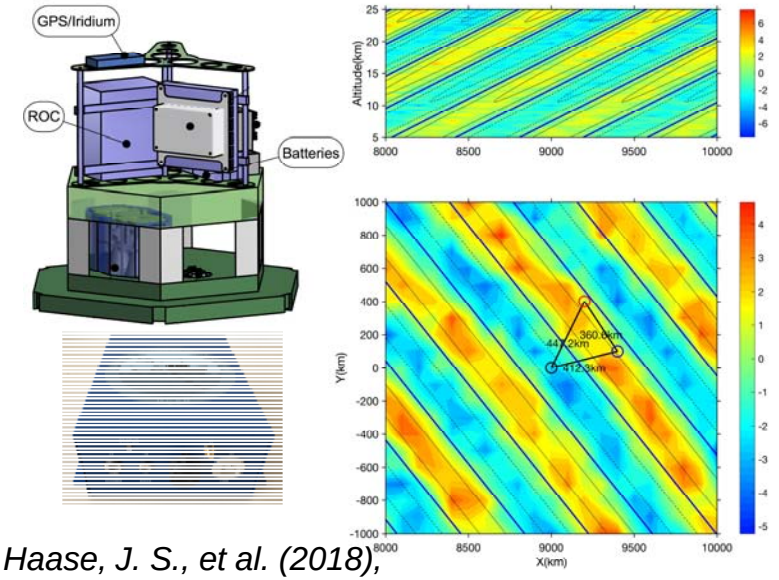

Haase, J. S., et al. (2018), Around the world in 84 days, EOS, 99.

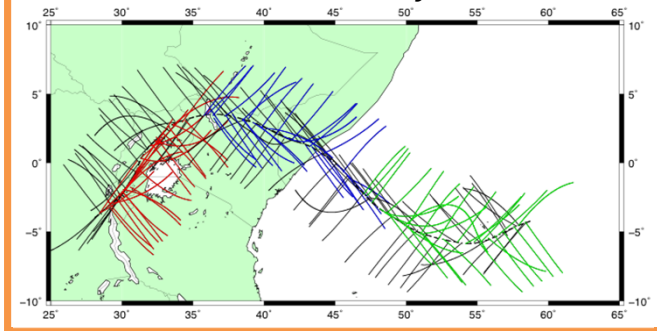

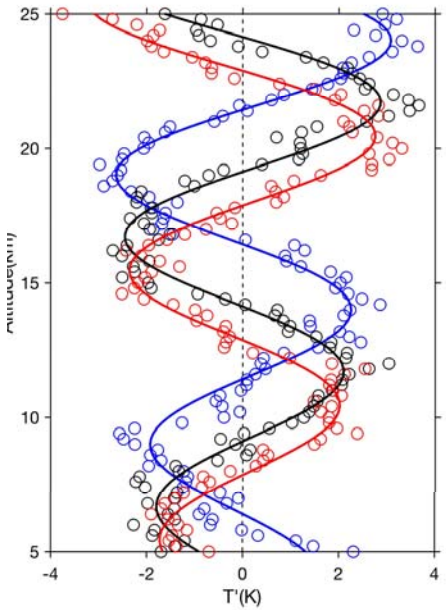

Reconstructed wave variation of temperature in cross-section and map view
Forward simulated temperature profiles at the three points shown in the map at left (solid lines) and retrieved temperature profiles from three radio occultation simulations (dots).

FLIGHTS STARTING 25 NOVEMBER 2019!!!

Potential for deployment on commercial aircraft

Flights in GTS database in one day
~3500 occultations over CONUS
11 Sept 2013 CO extreme flooding event
(Chen 2017; Gochis et al., 2015)

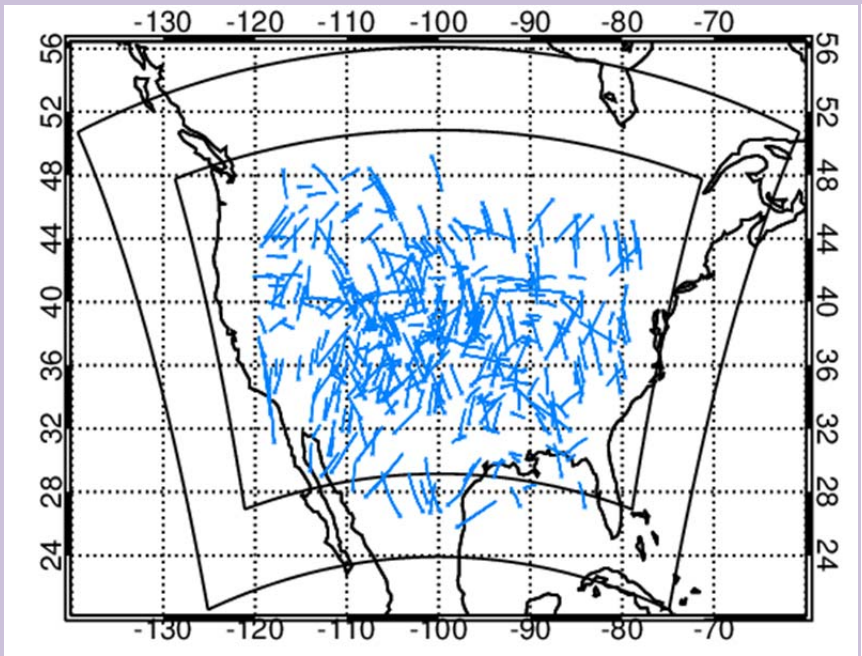

14 transatlantic AMDAR flights in one day
~250 occultations (GPS only)
(Lesne et al., 2002)

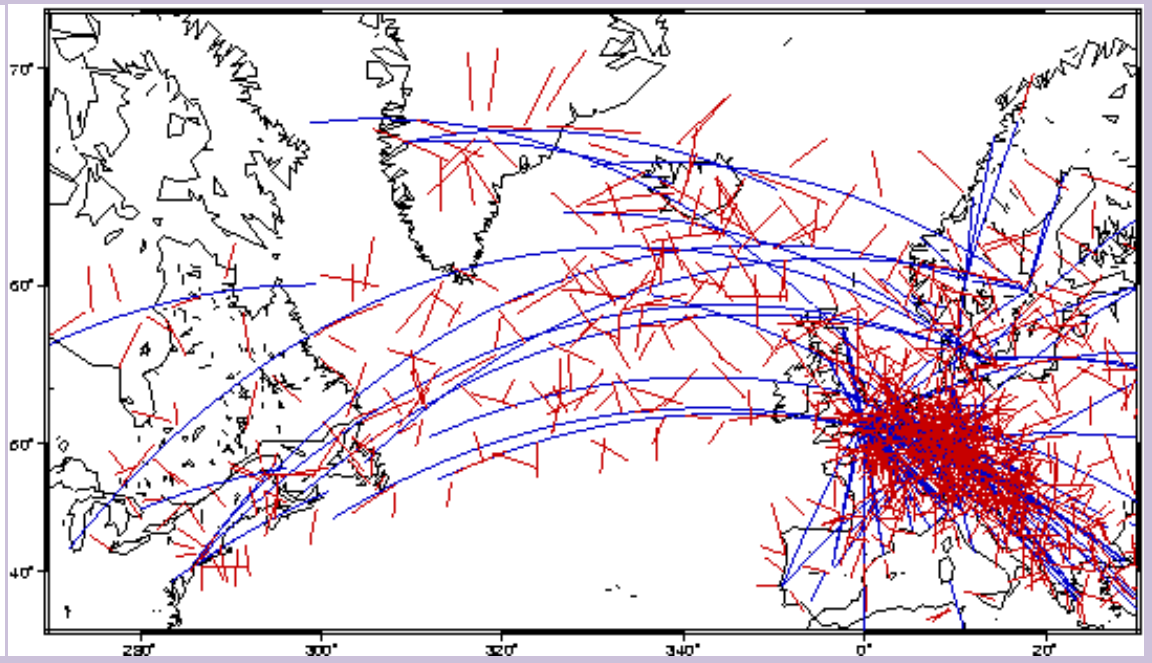

For mesoscale modeling case studies the variability in temporal sampling has a significant effect.

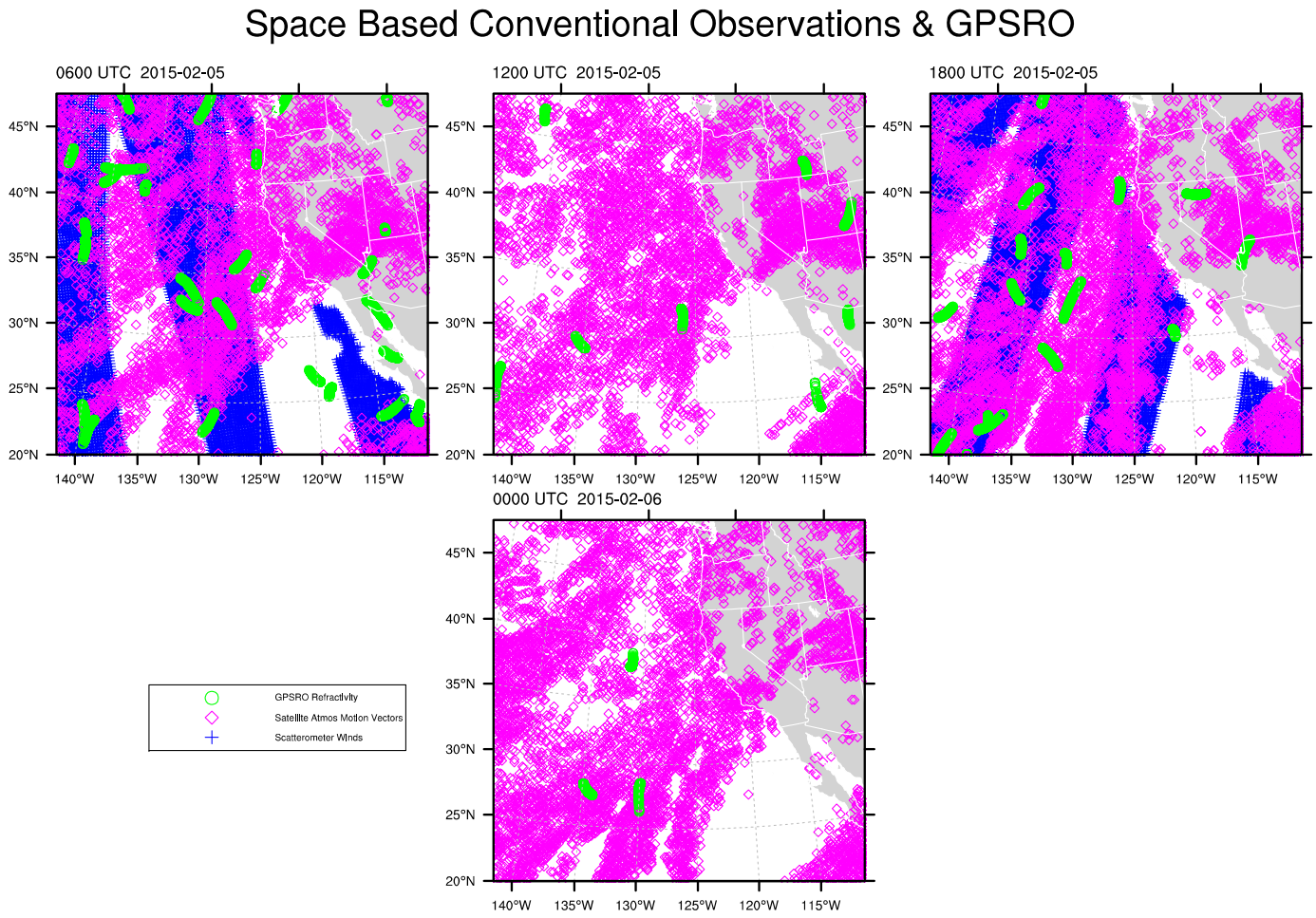

GSI/West-WRF DA system experiment

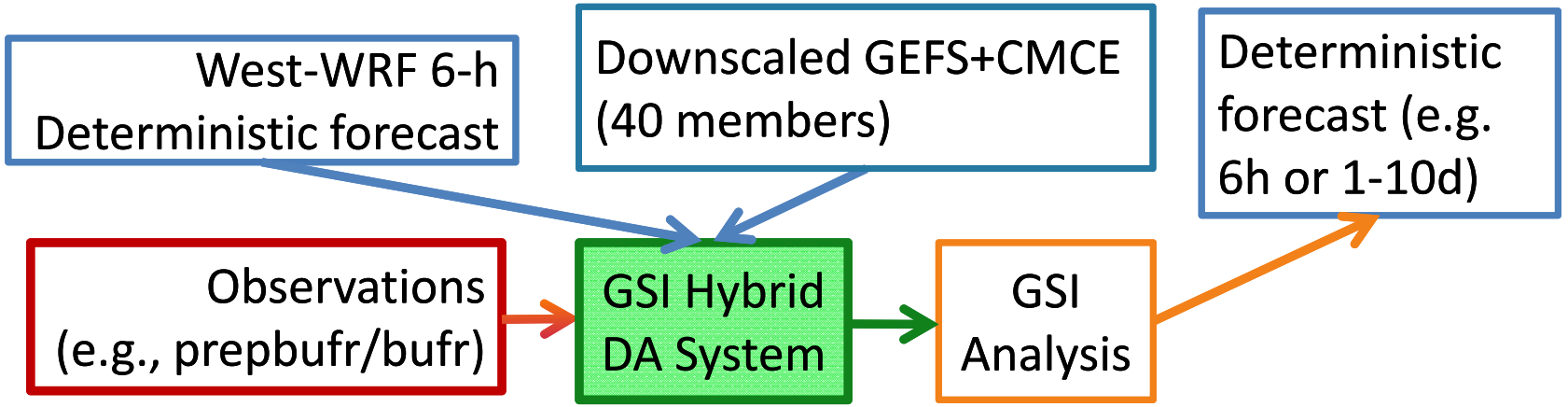

- West-WRF: version 3.9.1.1
- GSI: v3.6; hybrid 4DEnVar for data assimilation
- Ensembles are generated by downscaling GEFS ensemble (20 member) and CMCE ensemble (20 member).
- Observations assimilated: Conventional data in NCEP prepbufr, satellite atmospheric motion vector winds, GPSRO, with and without dropsondes

Validation of dropsonde data assimilation experiments

Atmospheric River offshore | **Landfall** | **NonAR cyclogenesis**

Landfall Oregon

Landfall Vancouver Is.

Experiments (Zheng)

26 Jan | 27 Jan | 28 Jan | 29 Jan

0:00 | 3:00 | 6:00 | 9:00 | 12:00 | 15:00 | 18:00 | 21:00 | 0:00 | 3:00 | 6:00 | 9:00 | 12:00 | 15:00 | 18:00 | 21:00 | 0:00 | 3:00 | 6:00 | 9:00 | 12:00 | 15:00 | 18:00 | 21:00 | 0:00 | 3:00 | 6:00 | 9:00 | 12:00 | 15:00 | 18:00 | 21:00

Initialization of background, boundary conditions from GFS forecast, run forward for 6 days + 6 hours

B/C B/C B/C B/C B/C B/C B/C B/C B/C B/C B/C B/C B/C

hybrid 4DEnVar data assimilation period, uses 7 x 1 hourly time steps

Free forecast (40 ensemble members + control fcst) for 6 days using updated analysis and B/C

D01 | D01 + D02

Observations

G-4 Flights RF01 2000 - 0200 Z

ARO Observations available for verification = 25 profiles

C-130 HI RF01 2000 - 0300 Z | RF02 2000 - 0300 Z

C-130 CA RF01 1900 - 0200 Z | RF02 1900 - 0200 Z

8 49 30 = 87 dropsondes total | 8 25 18 = 51 dropsondes

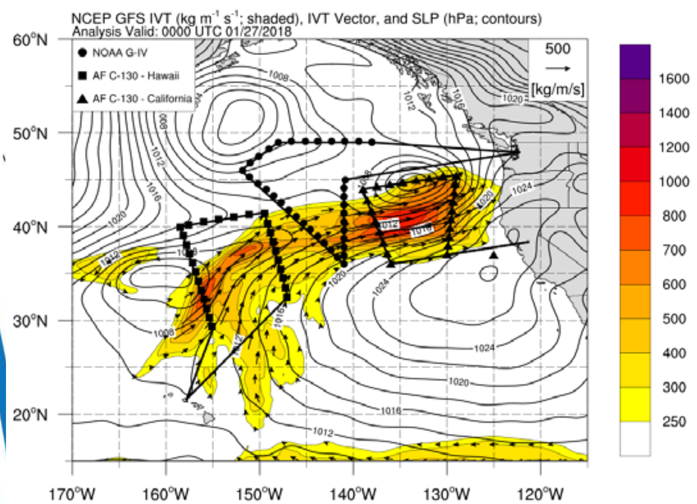

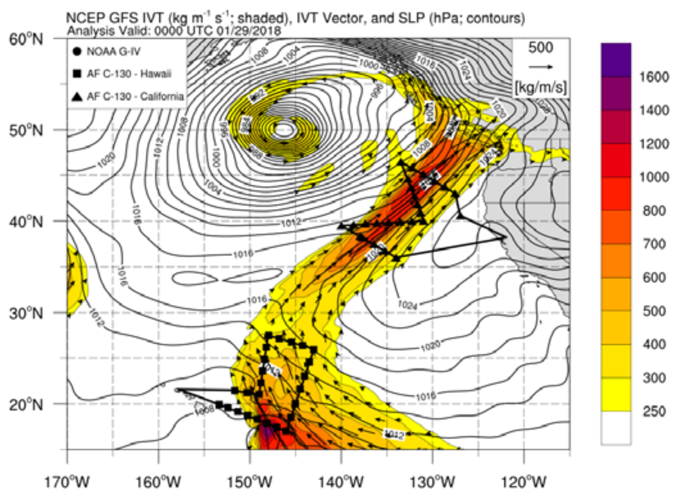

- ARO observations are available on 27 Jan 00Z to verify the analysis after dropsonde data assimilation
- Preliminary dropsonde data denial experiments comparing 4DEnVar and 3DEnVar
- (*Zheng et al., 2019, in prep.)*

Impacts of dropsondes (analysis drops – denial)

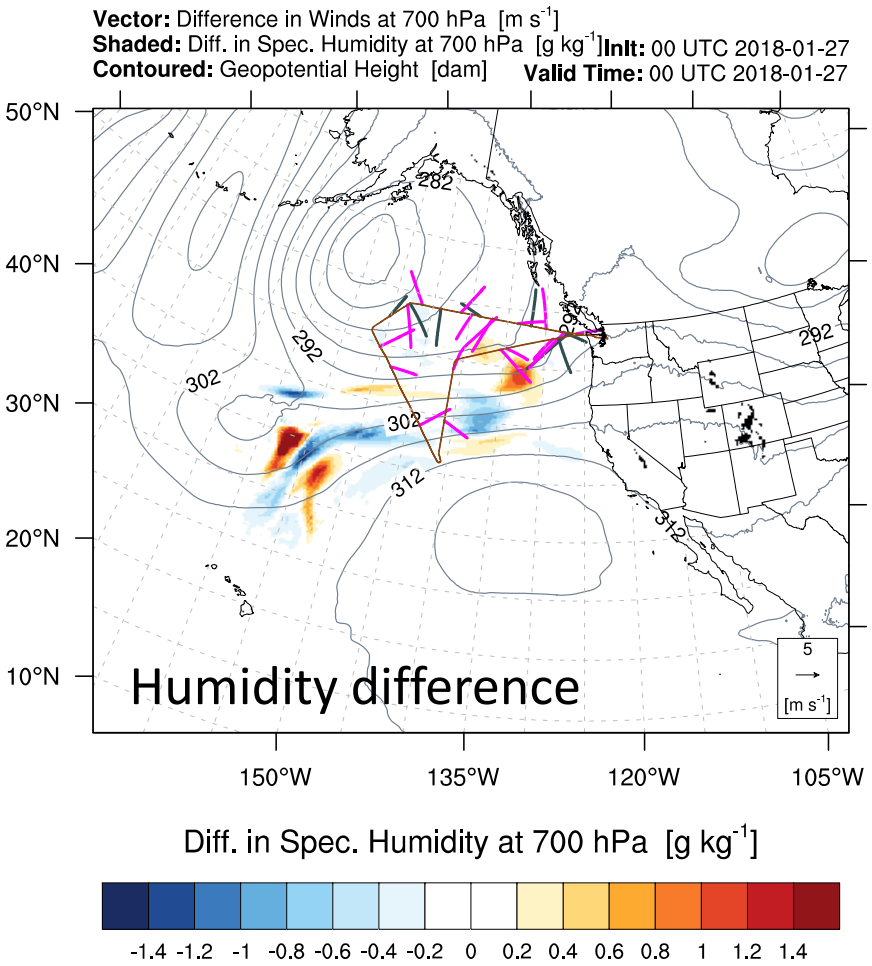

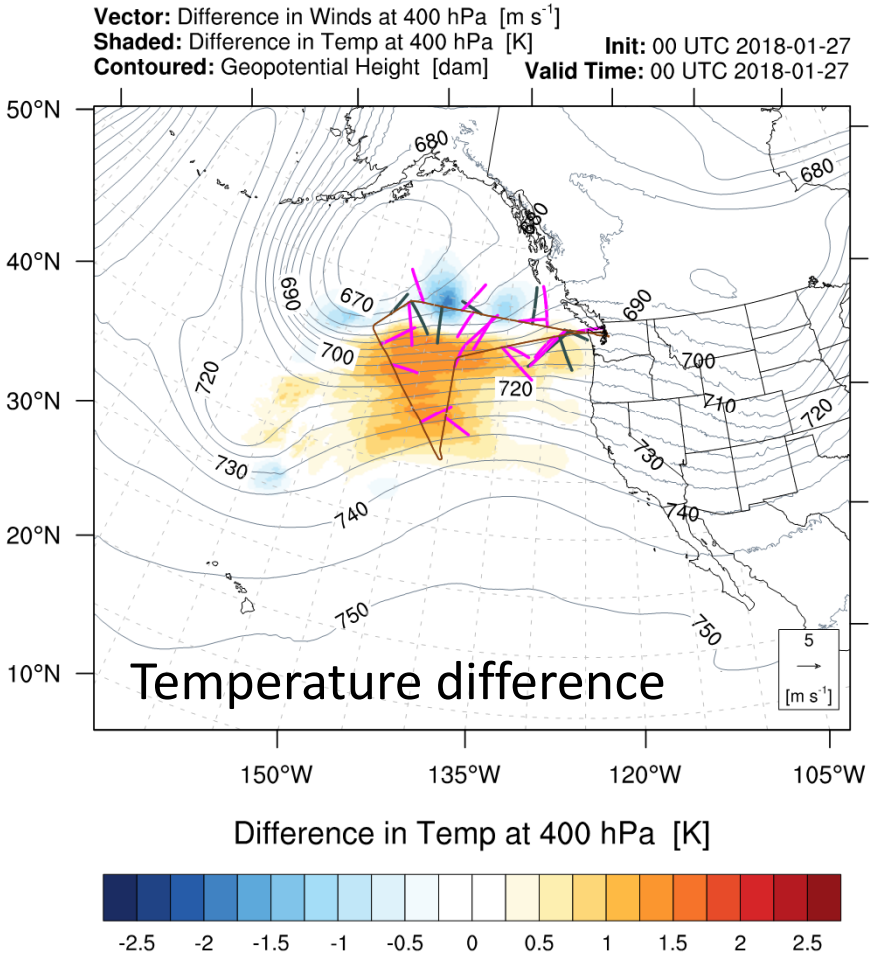

Results

- Drops vs no Drops
- Compare % differences in refractivity
- (ARO N – WRF N) / WRF N
- Drop experiment has lower bias than denial experiment
- RMS is mixed, sometimes higher, sometimes lower

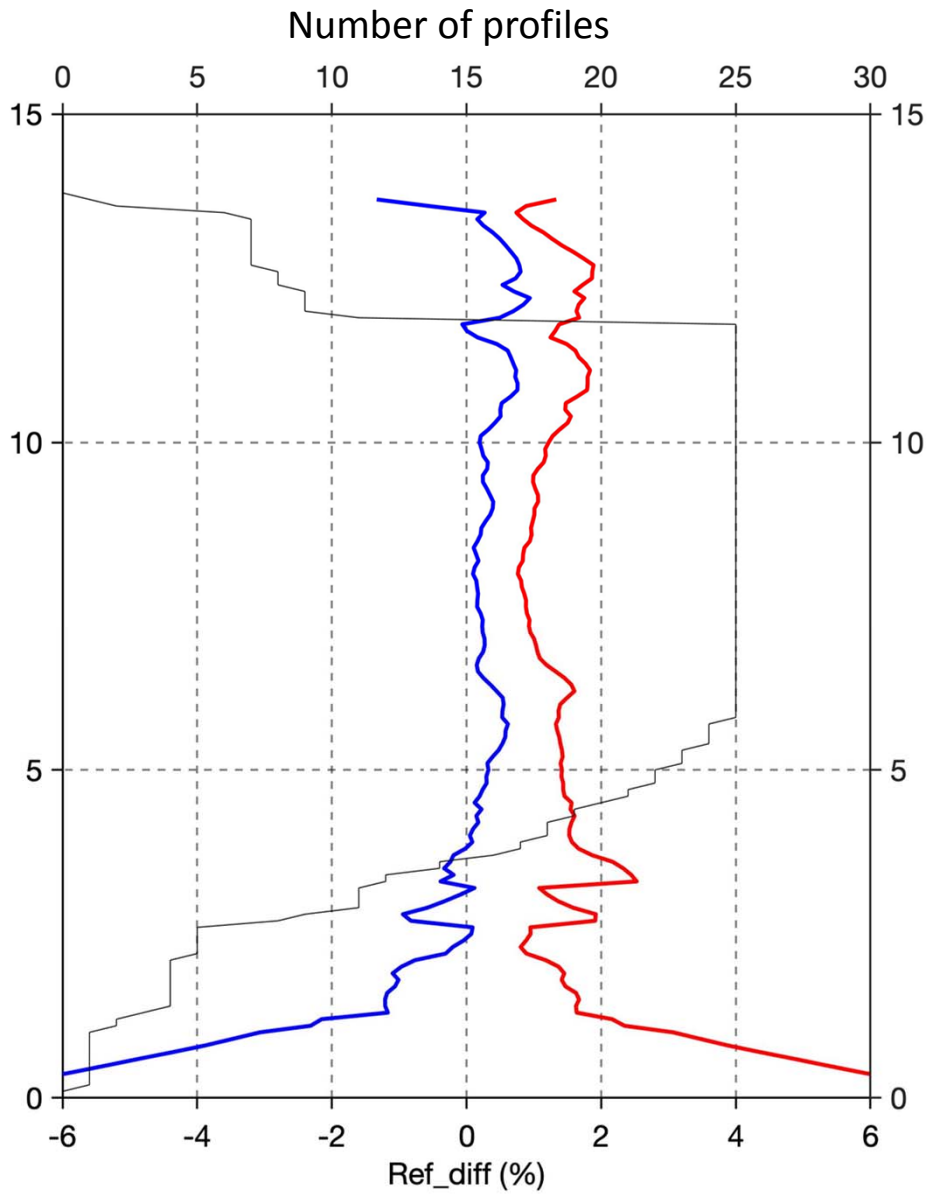

Results - ECMWF

- (ARO N – ECMWF N) / ECMWF N
- Drop experiment has smaller bias (~lower T) than ECMWF experiment from 7-12 km
- Drop experiment has larger bias (moister) than ECMWF experiment at ~3 km
- Drop experiment has lower RMS than ECMWF experiment from 6-12 km.

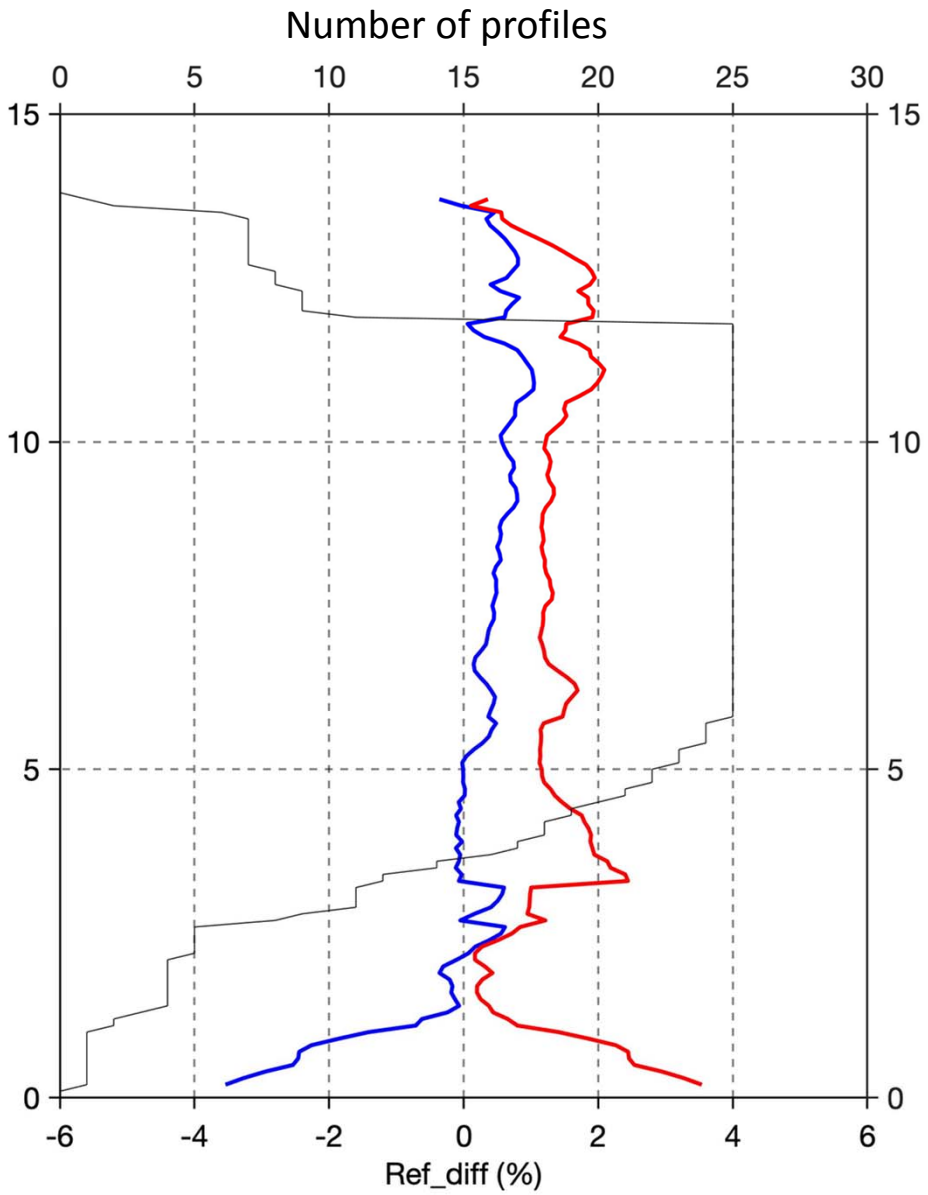

Northeastern Pacific Storms

- Major concern is sampling the moist low-level jet
- 37 profiles in domain
- 22 profiles extend below 1 km (relatively good percentage)
- 3 profiles below 0 km, but they are flagged with badness scores of 68, 526, and 1730, consistent with badness failing threshold.

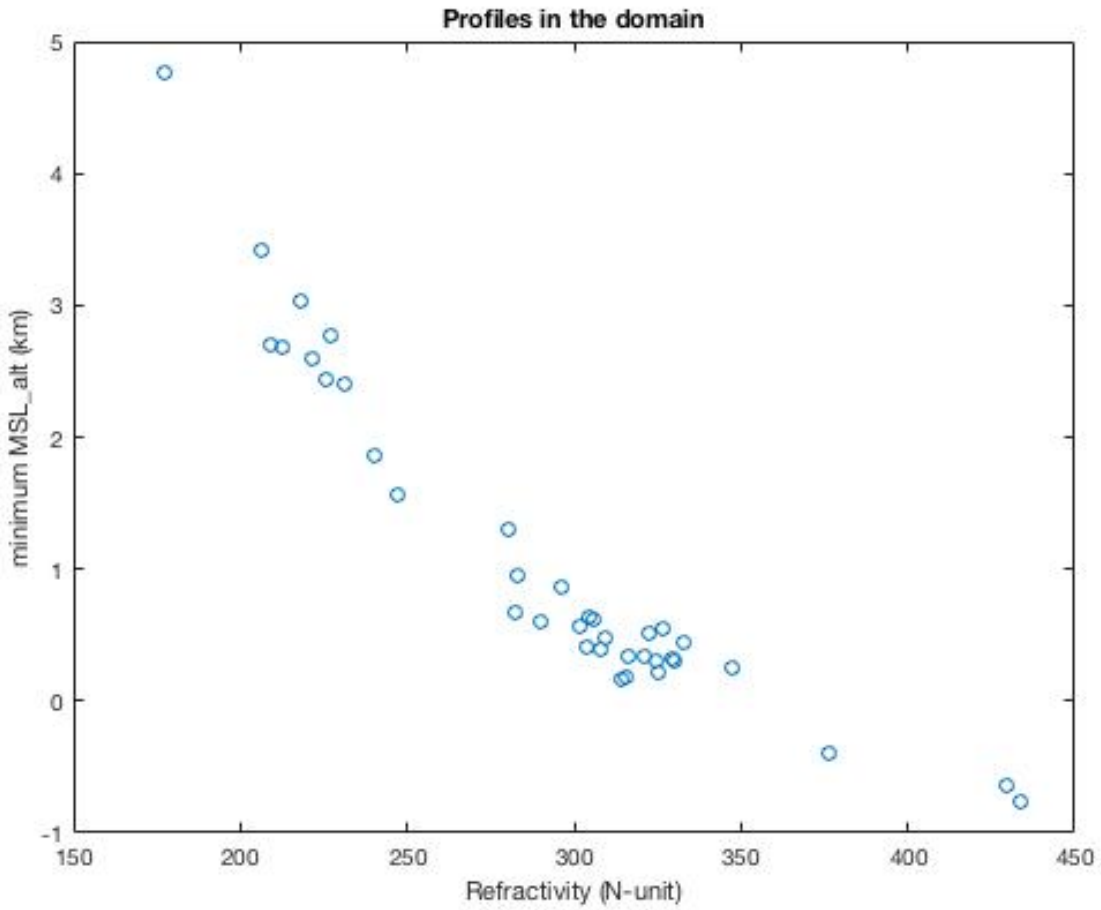

Study of IVT error for 2019 cases

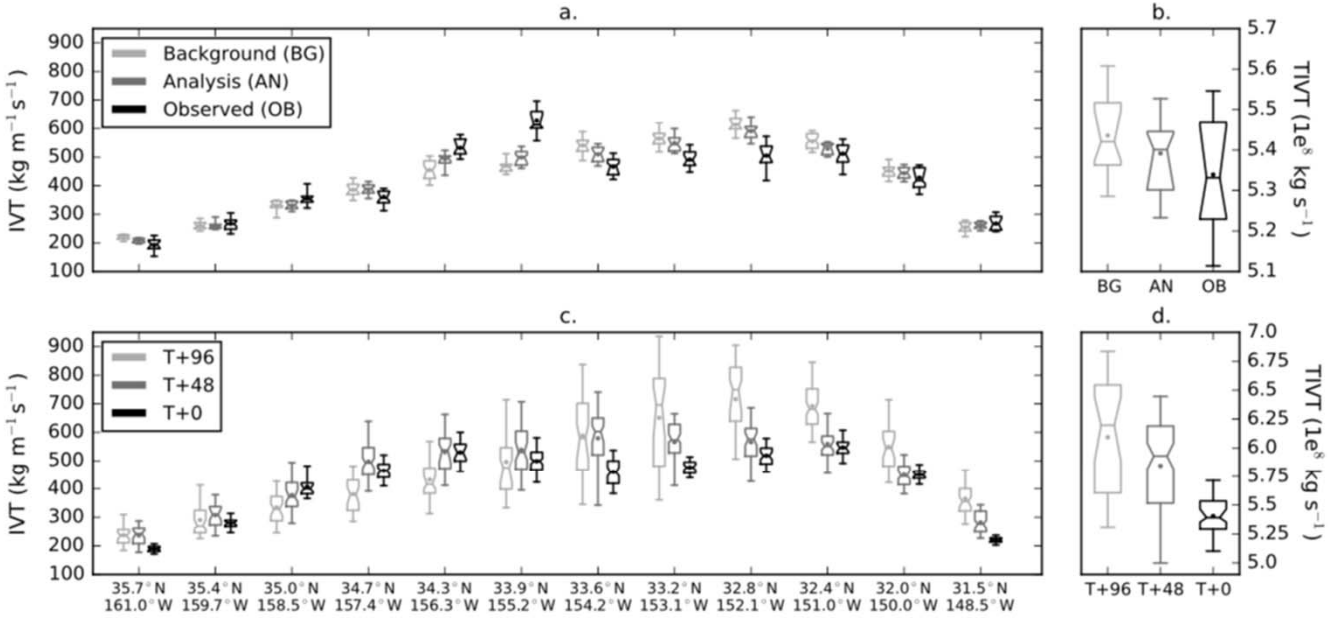

Figure 2. Example of an atmospheric river transect. (a) The integrated vapor transport (IVT) distribution in the 25 ensemble of data assimilations members of the background, analysis, and observation at each dropsonde across the atmospheric river (AR) as given by cyan dots in Figure 1d. (b) The distribution of the total IVT integrated across the AR. (c) The IVT distribution in the 50 ensemble members of the $T + 96$ forecasts, $T + 48$ forecasts, and $T + 0$ valid at 00UTC 3 February 2018. (d) The distribution of the total IVT integrated across the AR. The bottom and top of the boxes correspond to the 25th and 75th percentiles, respectively, the line in the box is the median, the dot in the box is the mean, and the whiskers represent the 5th and 95th percentiles. In the boxes, the notch shows the 95% confidence interval around the median from a 1,000 bootstrapped sample.

Lavers et al.,GRL, 2014

Study of IVT error for 2019 cases

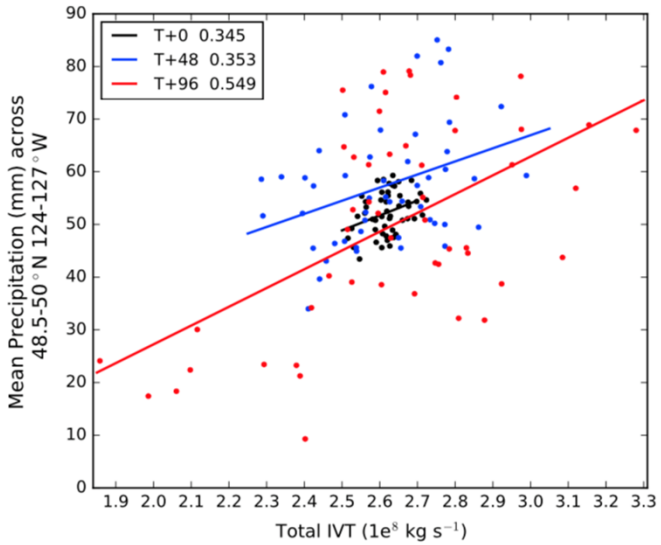

Figure 3. Relationship between integrated vapor transport (IVT) and rainfall in the 50 ensemble members. For IOP2, the total IVT flux valid at 00UTC 29 January 2018 averaged over the four transects nearest the North American Coast (Figure 1b) is plotted against the average model rainfall across southwestern Vancouver Island (48.5°N–50°N 124°W–127°W) valid for 00UTC 29 to 00UTC 30 January 2018. The black dots refer to IVT at $T + 0$ and rainfall accumulated from $T + 0$ to $T + 24$; the blue dots refer to IVT at $T + 48$ and rainfall accumulated from $T + 48$ to $T + 72$; the red dots refer to IVT at $T + 96$ and rainfall accumulated from $T + 96$ to $T + 120$. The linear regression lines are plotted, and the linear Pearson correlations (which are significant at the 0.05 level) are given in the legend.

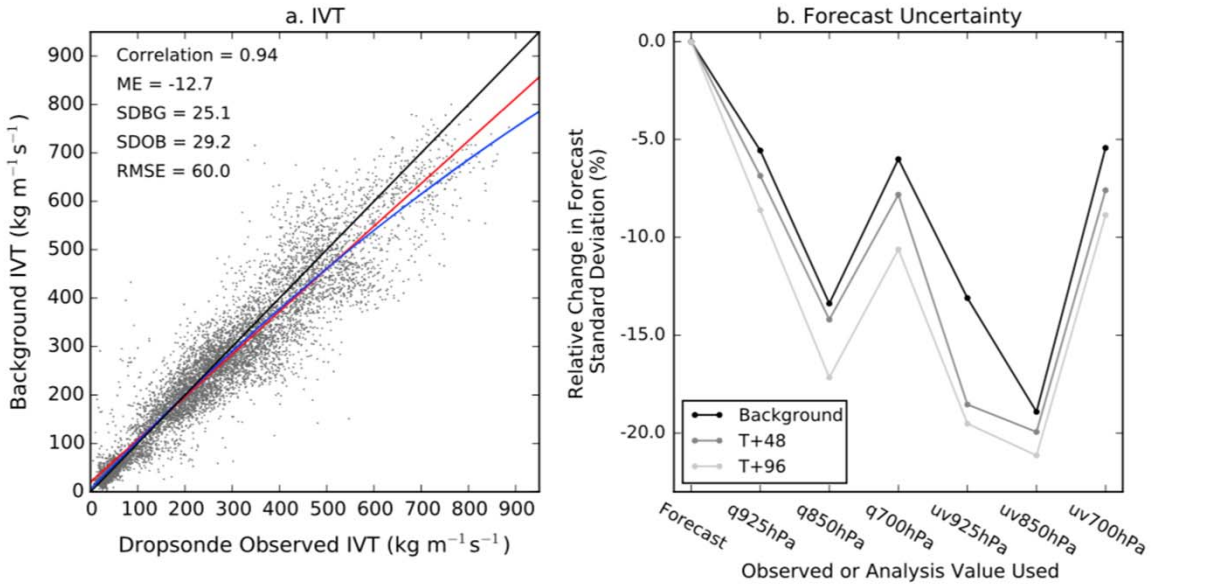

Figure 4. Uncertainty in integrated vapor transport (IVT) forecasts. (a) Scatterplot of the IVT in the 25 ensemble of data assimilations background and observed realizations at the 319 dropsondes (n = 7,975). The linear correlation, mean error (forecast-observed), standard deviation of the background forecasts, standard deviation of the perturbed observations, and the root-mean-square error are given. The 1:1 line is given in black, the linear regression line is in red, and the second degree polynomial line is in blue. (b) The relative change in IVT forecast standard deviation (%) compared to the forecast when replacing the forecast specific humidity q or winds uv at 925-, 850-, and 700-hPa levels with the unperturbed observation or unperturbed analysis value from the ensemble forecast system.

Lavers et al.,GRL, 2014

Center for Western Weather and Water Extremes

Atmospheric River Reconnaissance 2018

U.S. AIR FORCE

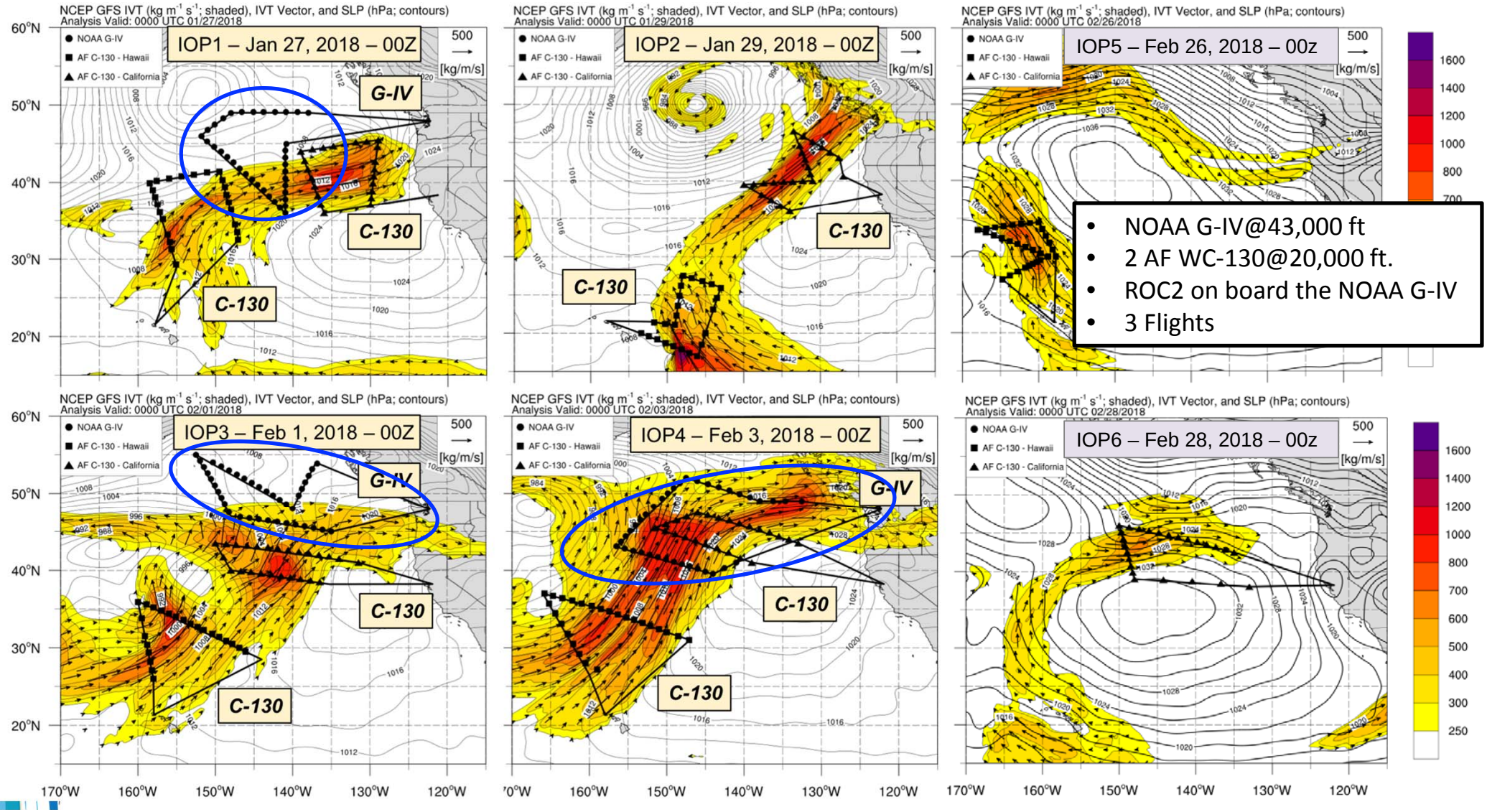

- NOAA G-IV@43,000 ft
- 2 AF WC-130@20,000 ft.
- ROC2 on board the NOAA G-IV
- 3 Flights

AR-2018: ROC2 receiver onboard the NOAA G-IV

ROC2

Septentrio PolaRx5

Applanix AV GPS/INS System

Anti-exposure suit in case of ditching in water

- 2015 campaign GNSS open-loop tracking – tracks to surface
- 2018, 2019 campaign simplified GNSS receiver – tracks to ~5 km
- Redundant recordings with two different GNSS receivers.
- Standard GPS antenna captures Galileo signals in the same frequency band.
- Acknowledgements: NOAA AOC

Sampling of the atmosphere by the GPS ray path

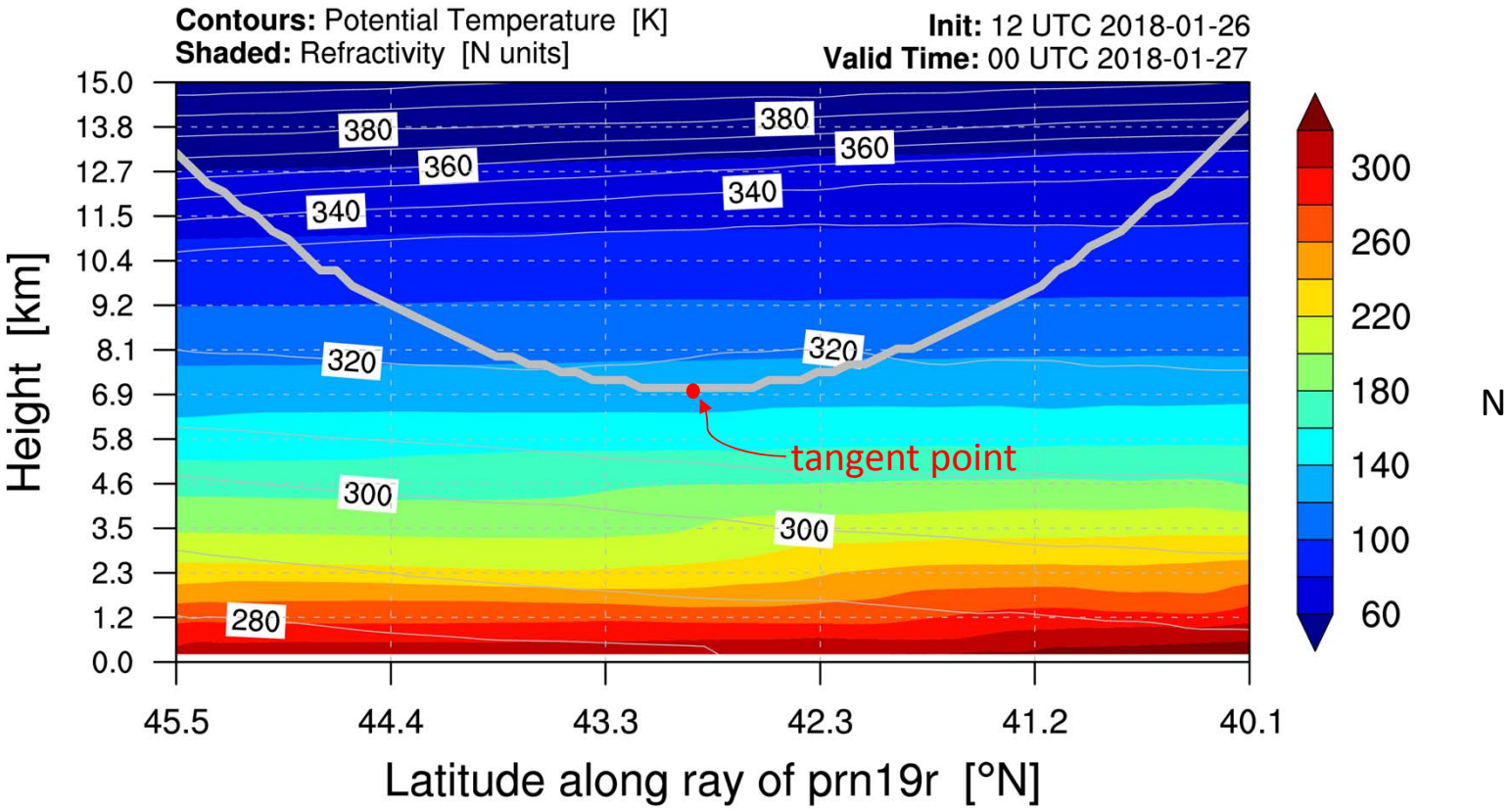

- Observations are most sensitive to N at the tangent point.
- The effect of refractivity in upper layers is removed in the retrieval process assuming horizontally constant values.
- Error in removing upper levels is due to the difference between the upper level N from a horizontally constant value.

Center for Western Weather and Water Extremes
SCRIPPS INSTITUTION OF OCEANOGRAPHY AT UC SAN DIEGO

UCLA

Jet Propulsion Laboratory
California Institute of Technology

Report: 20 Sept 2019

Assessment of the Coverage of GOES-16 Atmospheric Motion Vector (AMV) Winds in FV3GFS Relative to the Location of a Northeast Pacific Atmospheric River (AR)

Minghua Zheng and F. Martin Ralph (UC San Diego/SIO/CW3E), Bin Guan and Duane Waliser (UCLA and JPL/Caltech)

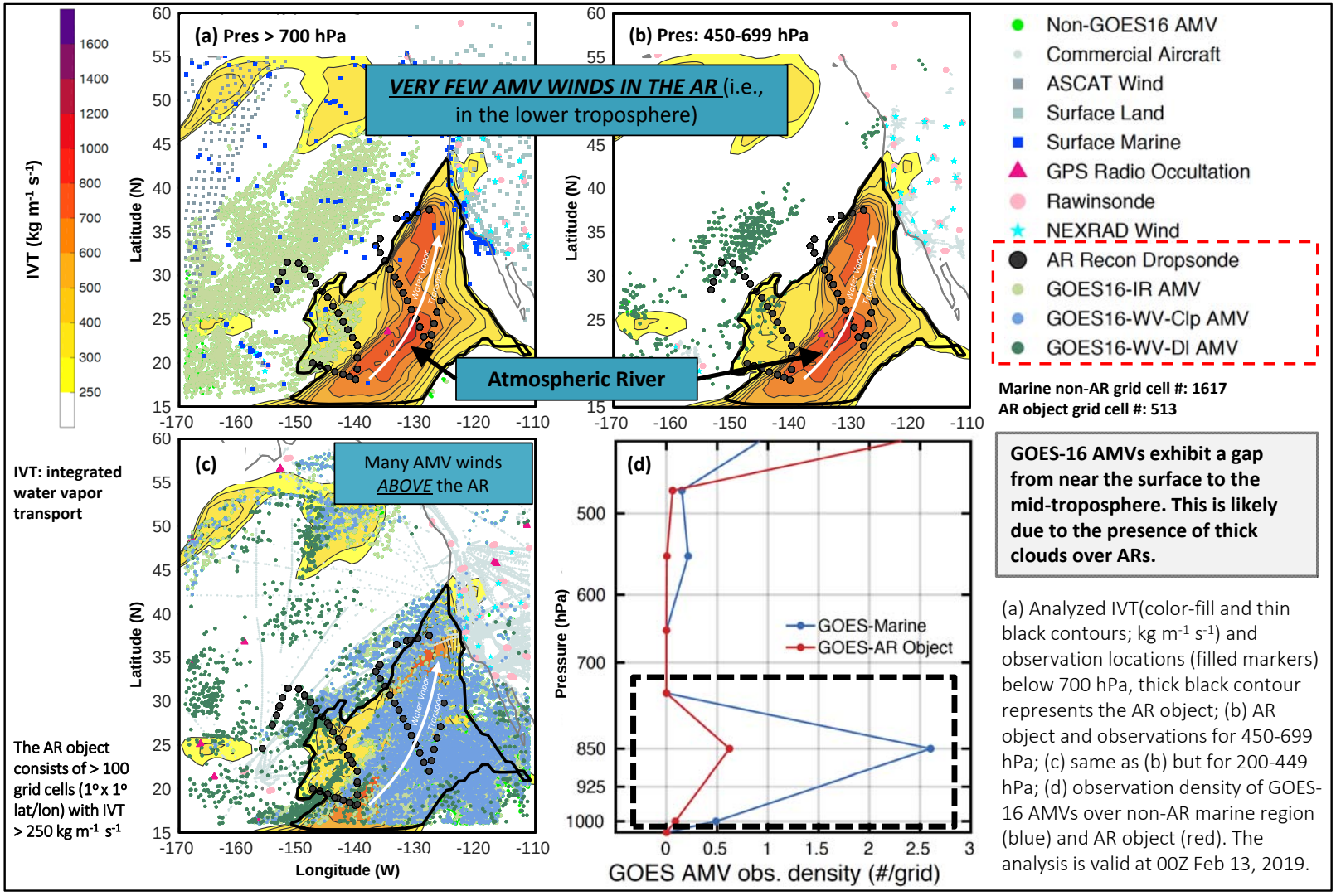

GOES-16 AMVs exhibit a gap from near the surface to the mid-troposphere. This is likely due to the presence of thick clouds over ARs.

(a) Analyzed IVT(color-fill and thin black contours; kg m^{-1} s^{-1}) and observation locations (filled markers) below 700 hPa, thick black contour represents the AR object; (b) AR object and observations for 450-699 hPa; (c) same as (b) but for 200-449 hPa; (d) observation density of GOES-16 AMVs over non-AR marine region (blue) and AR object (red). The analysis is valid at 00Z Feb 13, 2019.

Motivation: The AR region contains the greatest initial condition errors for west coast cyclone and precipitation forecasts. Although AMV winds from GOES-16 were intended to fill data sparse oceanic regions, no systematic evaluation of their coverage of ARs has been conducted. The goal of this preliminary study is to compare the spatial distribution of the GOES-16 AMV wind observations that were assimilated into FV3GFS, with the location of a NE Pacific AR sampled in "AR Recon" in 2019.

Finding: There were very few AMV winds in the AR object itself. Observation density in the AR in the lower troposphere is 20% of what is found at similar altitudes outside the AR in the marine region of the NE Pacific. **Key cause of the gap is that high clouds often overlay ARs, blocking VIS-, IR- & WV-satellite-based measurements.**

Implications: Additional observations, such as airborne dropsonde measurements, drifting buoys with pressure sensors, radio occultation (RO) observations (including satellite and airborne RO), better satellite-based winds (AEOLUS?) could help fill this critical gap.

Evaluation funded by NASA (GOES Special Task)

GPS / Galileo SNR Comparison

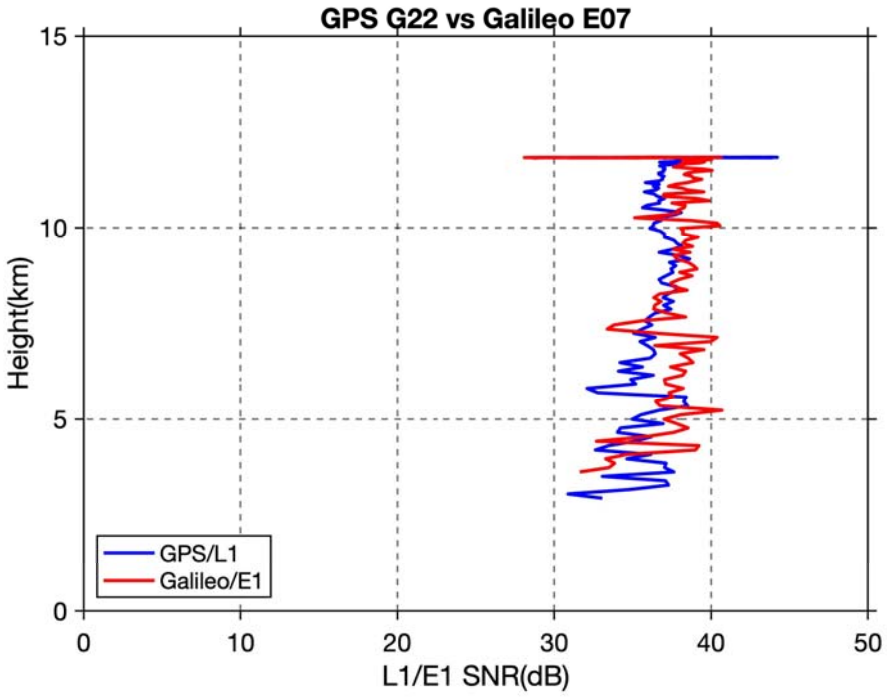

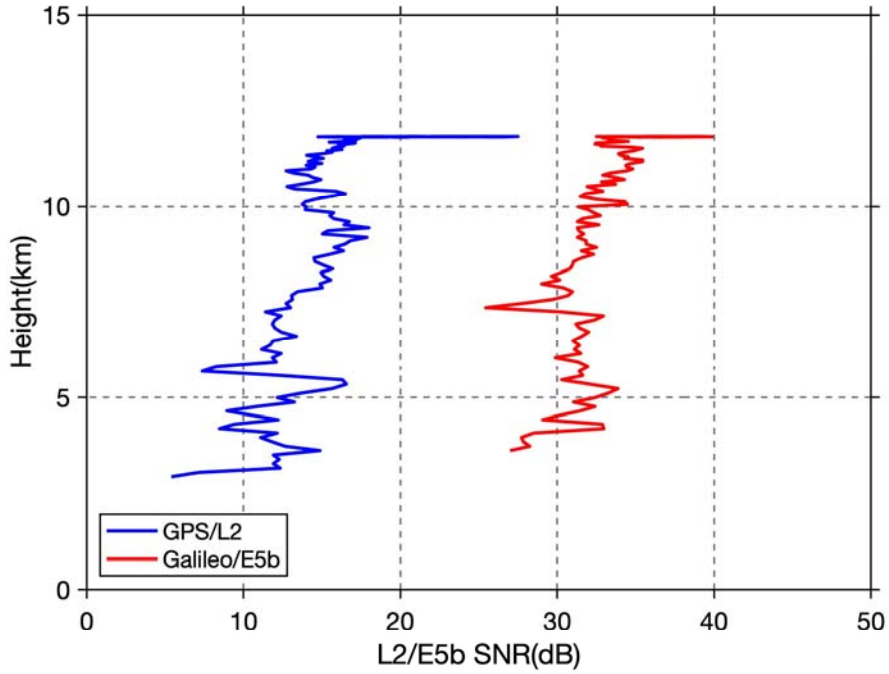

Example of poorly forecast high impact event

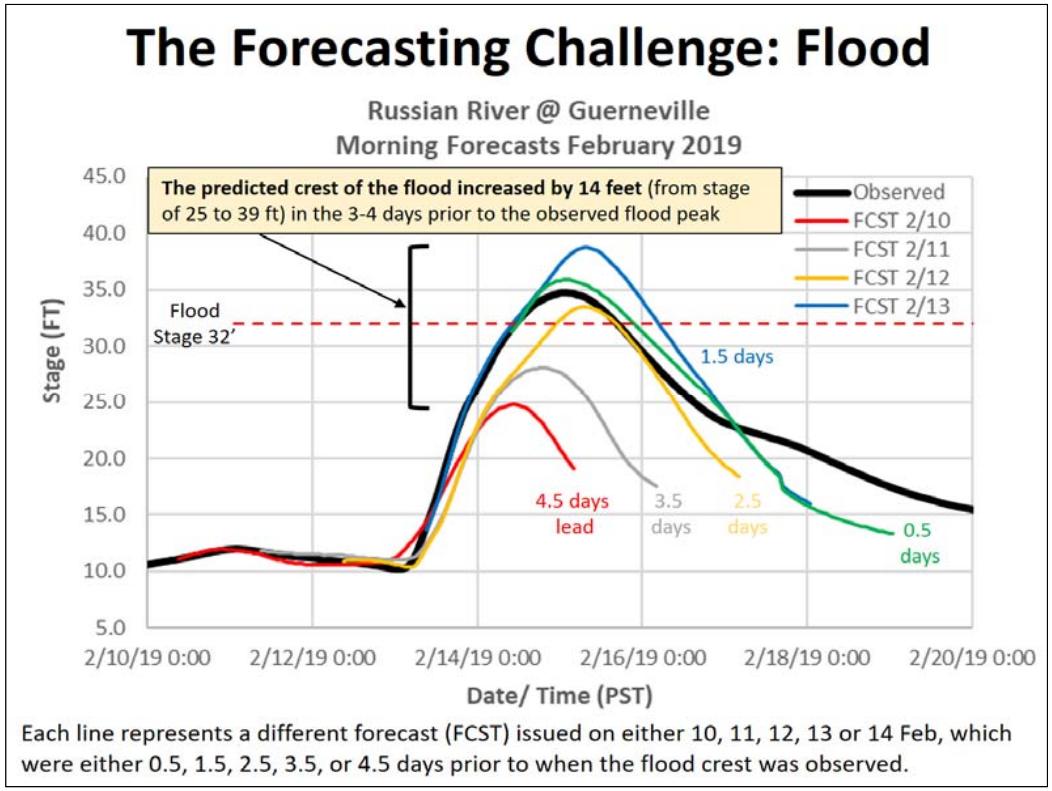

- 14 February 2019 northern California Russian River flooding
- Predicted flood crest changed by ~14 ft (4.5 m) over 3 days prior to the event
- (Sorry, I don't have ARO observations for this event)

Hydrostatic dry temperature on cold side

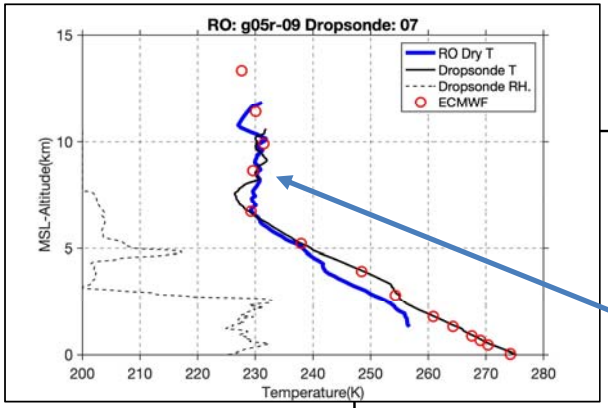

North of cold front, upper level temperature is nearly constant. ~~ARO detects a colder~~ temperature inversion at 7 km.

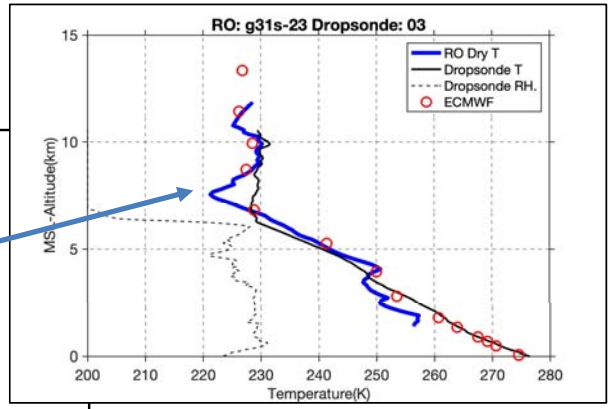

GPS

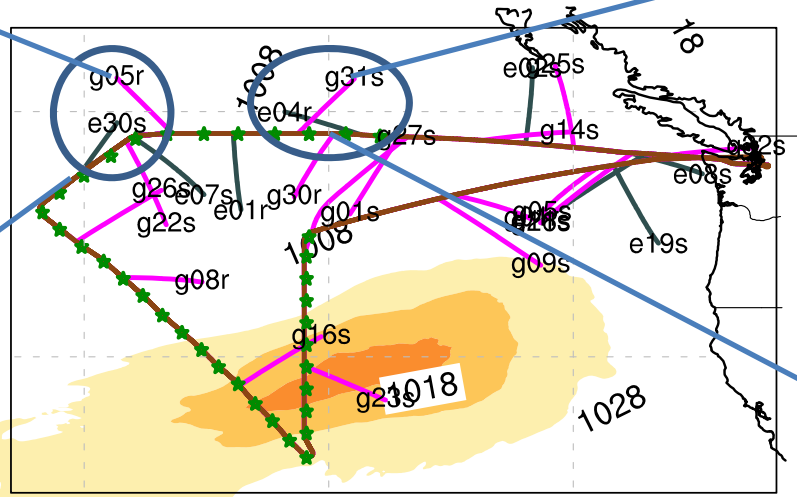

ECMWF analysis assimilates the dropsonde data, so agrees well.

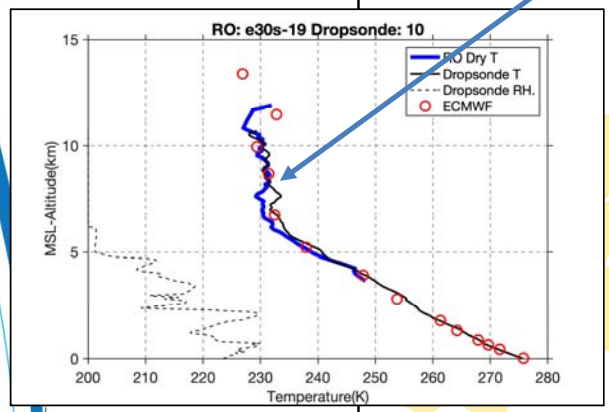

Galileo

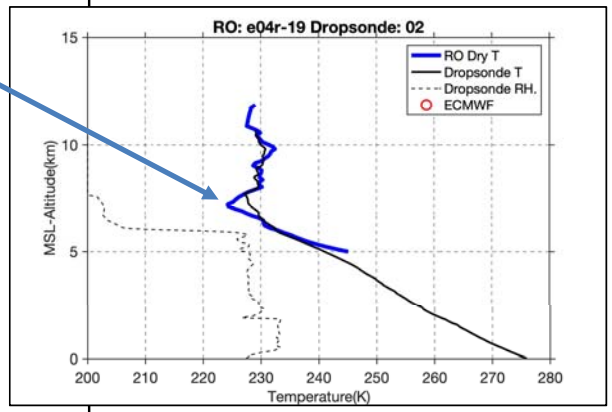

Hydrostatic dry temperature on warm side

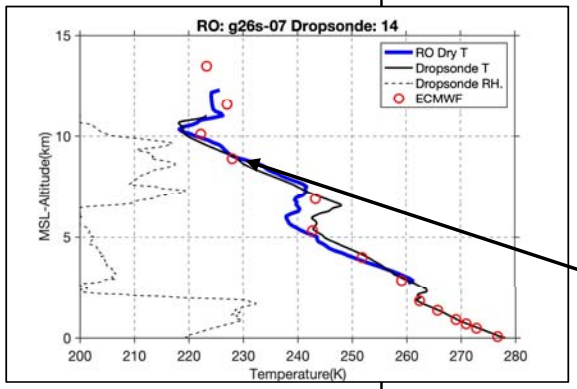

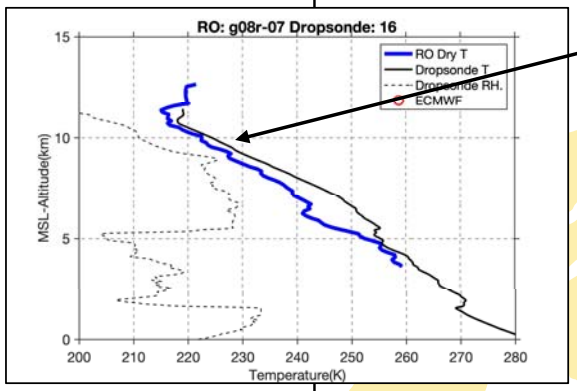

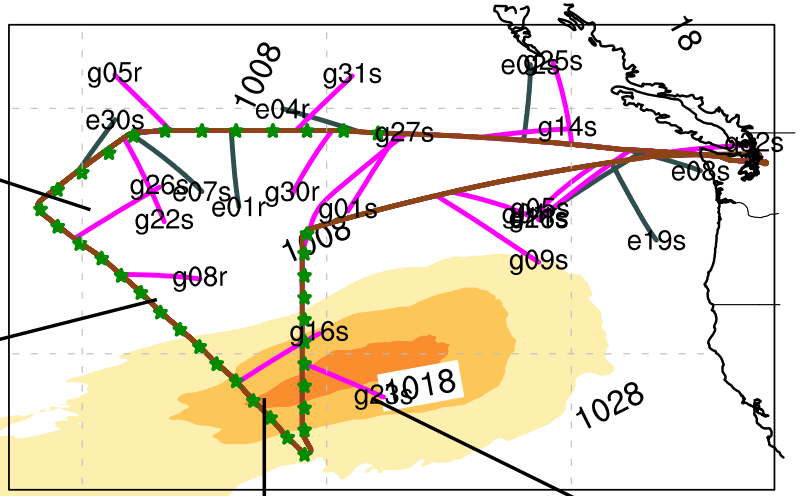

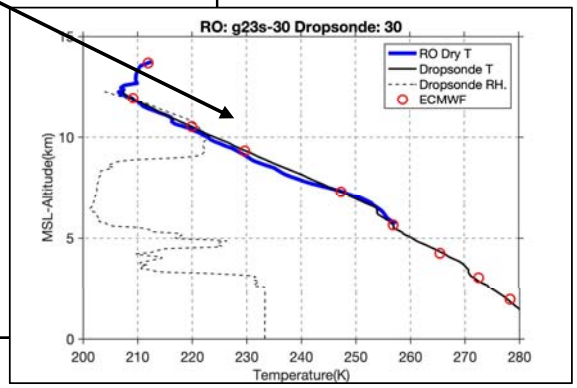

South of cold front, ARO captures steep upper level temperature gradient.

Fewer profiles on warm side, as expected for closed loop receivers, due to multipath.

Research challenge: forecast sensitivity methods

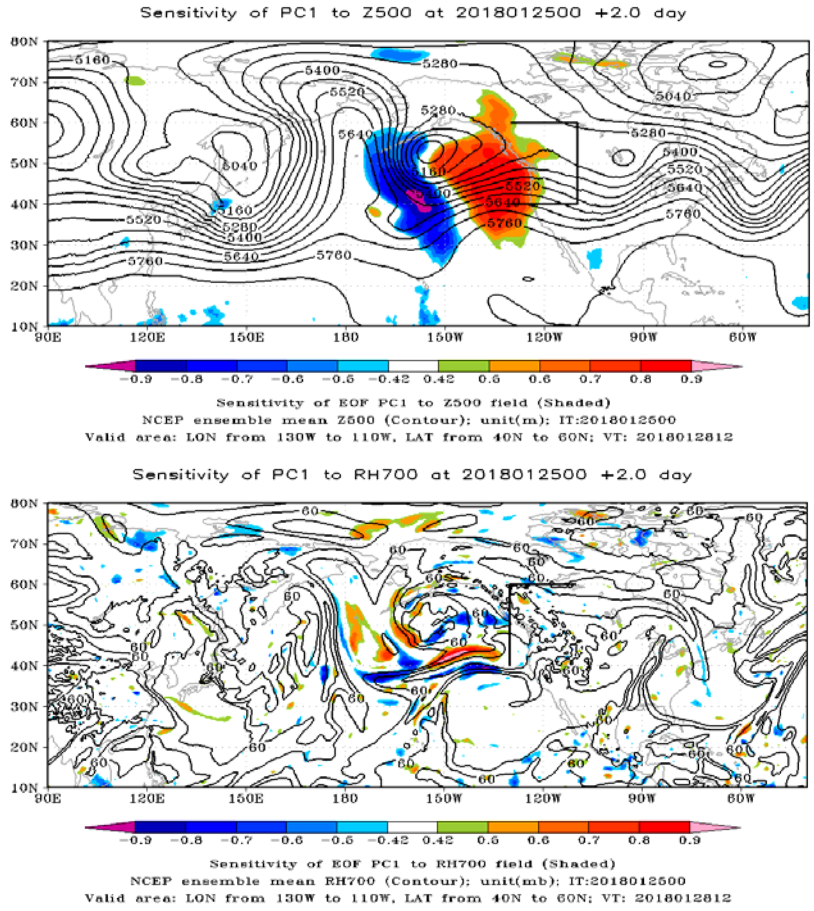

Zheng et al., 2013, Ensemble Sensitivity Tools for Assessing Extratropical Cyclone Intensity and Track Predictability, *Weather and Forecasting*

- Left shows the adjoint sensitivity of the 1st principle component of the variance of sea level pressure in the rectangle forecast for 12Z 28 January (24-36h after flight time) to Z500 at flight time 00Z 27 Jan
- A positive change in Z500 at the near the NOAA flight will produce a positive change in precipitation.
  - Forecast variable, observation variable?
  - Where to put the box?
  - Lead time? Changes every day
  - Confidence in scale of target sensitive area?